AD-A073 492 NAVAL OCEAN SYSTEMS CENTER SAN DIEGO CA F/G 17/1
SOME UNDERWATER PROPAGATION STUDIES IN THE VICINITY OF THE NOSC--ETC(U)
JUN 79 J NORTHROP
UNCLASSIFIED NOSC/TR-424 NL

| OF |
AD
A073492

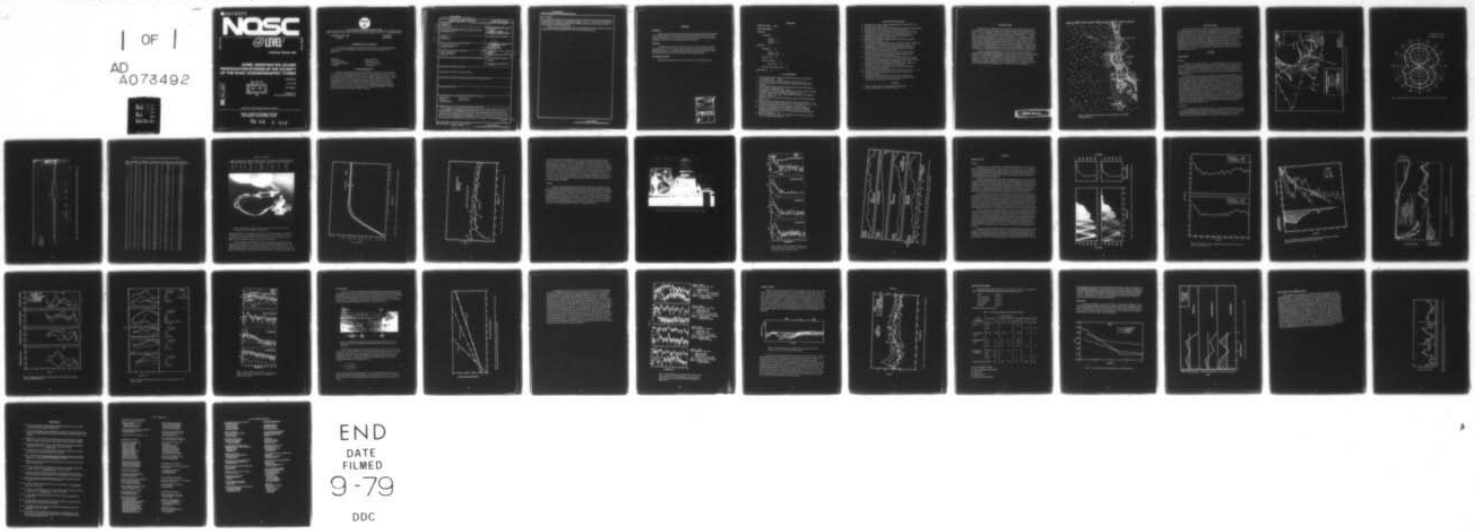

END
DATE
FILMED
9-79
DDC

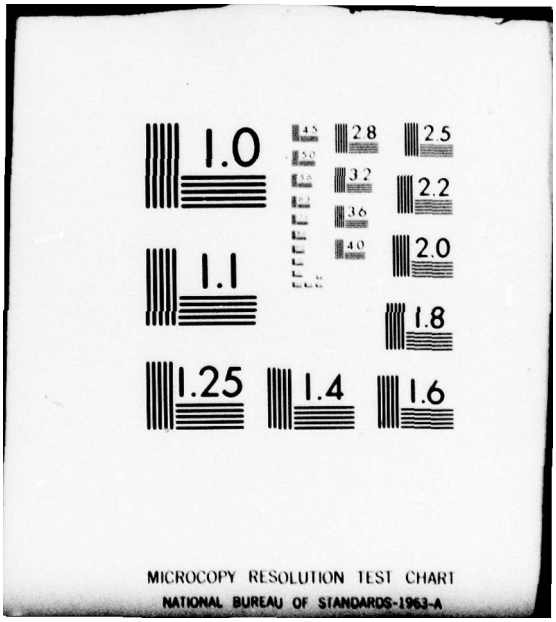
1.0
1.1
1.25
1.4
1.6
1.8
2.0
2.2
2.5
2.8
3.2
3.6
4.0
MICROCOPY RESOLUTION TEST CHART
NATIONAL BUREAU OF STANDARDS-1963-A

NOSC

NOSC TR 424

NOSC TR 424

Technical Report 424

SOME UNDERWATER SOUND PROPAGATION STUDIES IN THE VICINITY OF THE NOSC OCEANOGRAPHIC TOWER

J Northrop

June 1979

Final Report

Prepared for
Office of Naval Research

Approved for public release; distribution unlimited

NAVAL OCEAN SYSTEMS CENTER
SAN DIEGO, CALIFORNIA 92152

NAVAL OCEAN SYSTEMS CENTER, SAN DIEGO, CA 92152

AN ACTIVITY OF THE NAVAL MATERIAL COMMAND

SL GUILLE, CAPT, USN
Commander

HL BLOOD
Technical Director

ADMINISTRATIVE STATEMENT

The work reported herein was sponsored by the Office of Naval Research (program element 61153N, project RR03201) and conducted over the period August 1978 to March 1979.

Released by
EB Tunstall, Head
Environmental Acoustics
Division

Under authority of
JD Hightower, Head
Environmental Sciences
Department

ACKNOWLEDGEMENT

This work was supported in part by NAVELEX Code 320 and in part by the Office of Naval Research, Earth Physics Branch (Code 463). Recording and analysis of the data were done by T. E. Sixrud (NOSC). John Shepphard (SDSU) assisted in the work. F. Shipp and W. Friedl (NOSC) did the shooting. Dr. Homer P. Bucker (NOSC) provided advice, encouragement, and support. Instrumentation was provided through contracts with NAVELEX Code 320. The Naval Research Laboratory funded the CW tow experiments under the direction of S. Wolf. J. Olson and D. Good (NOSC) provided liaison between the various groups and assisted in the scheduling of the USNS DE STEIGUER. The SUS charges were obtained from ONR by CDR J. E. Minard.

UNCLASSIFIED

SECURITY CLASSIFICATION OF THIS PAGE (When Data Entered)

REPORT DOCUMENTATION PAGE

READ INSTRUCTIONS BEFORE COMPLETING FORM

1. REPORT NUMBER: NOSC TR-424
2. GOVT ACCESSION NO.:
3. RECIPIENT'S CATALOG NUMBER:

4. TITLE (and Subtitle): Some Underwater Propagation Studies in the Vicinity of the NOSC Oceanographic Tower
5. TYPE OF REPORT & PERIOD COVERED: Final Report - August 1978 - March 1979
6. PERFORMING ORG. REPORT NUMBER:

7. AUTHOR(s): John Northrop
8. CONTRACT OR GRANT NUMBER(s):

9. PERFORMING ORGANIZATION NAME AND ADDRESS: Naval Ocean Systems Center, San Diego, CA 92152
10. PROGRAM ELEMENT, PROJECT, TASK AREA & WORK UNIT NUMBERS: 61153N; RR03201; RR0320101; 531-MA17

11. CONTROLLING OFFICE NAME AND ADDRESS: Office of Naval Research, Arlington, VA 22217
12. REPORT DATE: June 1979
13. NUMBER OF PAGES: 38

14. MONITORING AGENCY NAME & ADDRESS (if different from Controlling Office):
15. SECURITY CLASS. (of this report): Unclassified
15a. DECLASSIFICATION/DOWNGRADING SCHEDULE:

16. DISTRIBUTION STATEMENT (of this Report)

Approved for public release; distribution unlimited.

17. DISTRIBUTION STATEMENT (of the abstract entered in Block 20, if different from Report)

18. SUPPLEMENTARY NOTES

19. KEY WORDS (Continue on reverse side if necessary and identify by block number)

Propagation loss
Seismic waves
Acoustic attenuation
Marine geology
Acoustic modeling

20. ABSTRACT (Continue on reverse side if necessary and identify by block number)

Low-frequency (< 50 Hz) underwater sound transmission studies were made to a range of 81 km west of the NOSC oceanographic tower off Mission Beach, San Diego, California. Both explosive and CW sources were used to ranges of 26 km, and explosive sources to longer ranges. Both hydrophones and three-component geophones were used as detectors. Results show that the propagation is better in the E-W direction, but that the noise level is higher. Thus, on the continental shelf, the N-S geophones appear to be the best detectors for sounds below 20 Hz; but at longer ranges, the hydrophones have a better S/N ratio. At close range (< 5 km) propagation modes appear

(Continued)

DD FORM 1 JAN 73 1473 EDITION OF 1 NOV 65 IS OBSOLETE
S/N 0102-LF-014-6601

UNCLASSIFIED

SECURITY CLASSIFICATION OF THIS PAGE (When Data Entered)

393 159

20. (Continued)

to be controlled by the thickness of the unconsolidated sediment. The ground arrivals indicate a semiconsolidated sedimentary layer 553 m thick with a compressional wave speed of 4770 m/s. A second arrival line, having a sound speed of 3420 m/s, is interpreted as a shear wave that traveled in the basement rock and was converted back to a compressional wave before reaching the surface.

Overall, there was no outstanding difference between the hydrophone and geophone detectors, except the geophones do have a directionality gain of about 5 dB over omnidirectional sensors.

SUMMARY

PROBLEM

Conduct very-low-frequency underwater sound propagation experiments in shallow water off Mission Beach, CA, to measure the S/N ratio on both hydrophones and three-component geophones for narrowband (CW) and wideband (explosive) sources. Model the propagation loss by means of a normal mode computer program.

RESULTS

The geophones had a better S/N ratio for close-in shots (less than 10 miles) at frequencies below 15 Hz. At longer range (and deeper water), the hydrophone outperformed the geophones. Propagation loss was modeled successfully by means of a Fast Field Program modified to run on the UNIVAC 1110 computer at NOSC.

RECOMMENDATIONS

Make similar measurements and/or calculations in area of strategic interest.

CONTENTS

ILLUSTRATIONS

ILLUSTRATIONS (Continued)

TABLES

INTRODUCTION

Propagation of low-frequency sound in shallow water involves interaction with the bottom and, in general, the longer the wavelength, the deeper the penetration of the bottom. Thus, the possibility of detecting sounds from ships transiting the continental shelf – where the water is generally less than 100 fathoms (182.88 m) deep – by using geophones buried in the sediment is an attractive one (Refs. 1,2). Geophones are instruments which, like seismometers, are sensitive to particle motion in the ground. Detection by this means is especially rewarding for sounds below the "cutoff" frequency, the frequency below which wavelengths are too long to permit propagation in the water layer. The sea floor in the shallow-water areas of the world varies considerably in thickness and composition. Thus, propagation loss varies as a function of geographic location as well as of frequency and seasonal changes in the sound-speed profile of the water layer (Ref. 3)

In order to measure propagation loss and the relative reception capability of geophones and hydrophones off San Diego, a program to install an array of bottom-mounted detectors near the NOSC oceanographic tower was funded in 1977 by NAVELEX 320 (Fig. 1). Ambient noise and 50-Hz CW measurements were made with this array in August of 1978, and an explosive beyond the break in slope was made under ONR (Code 463) sponsorship in December 1978. An additional CW tow was made in February 1979 for NRL. This report summarizes some of the results of these experiments.

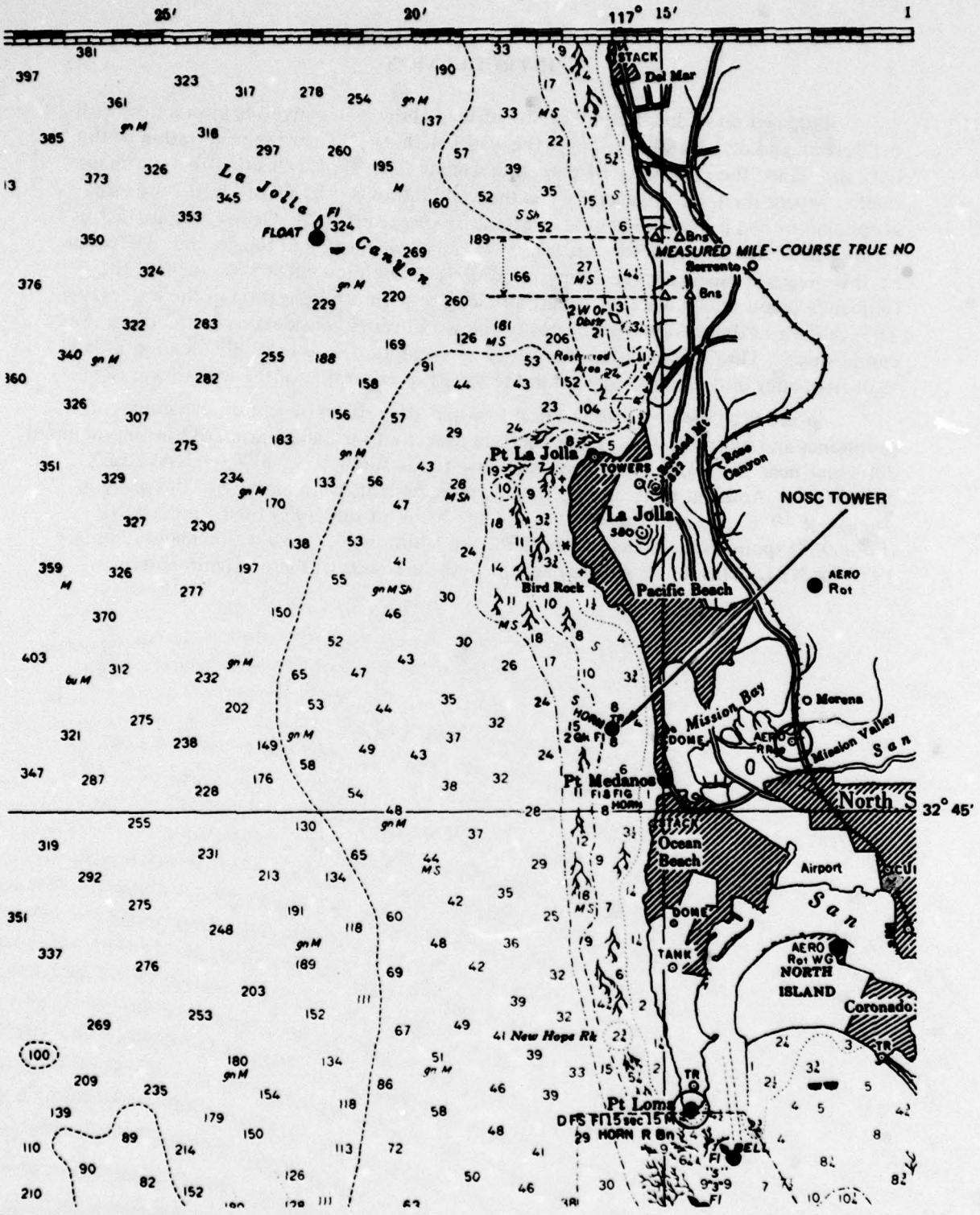

Figure 1. Map of the San Diego, California, area showing the location of the NOSC oceanographic tower.

PREVIOUS WORK

Early work on detection of sound by geophones was done at the Hudson Laboratories of Columbia University in the early 1950's. Several 1956-ft (596.18-m) wells were drilled to basement (granite rock) on Fire Island at the Bellport, NY, coast Guard Station (Ref. 4) and vertical geophones were inserted in a well at various depths from 300 ft (91.44 m) to the bottom. Reception of both CW and explosive sources was completed to a range of about 10 miles (18.52 km) in three directions. Results showed recording in the wells was noisy, principally because of the excitation of organ pipe modes or "tube waves" (Ref. 3). Additional work was done off Florida by Urick (Ref. 5), McLeroy (Ref. 6), and Latham (as reported by Hecht in Ref. 2). Geoacoustic parameters of the NOSC tower site were reported in Ref. 7 and this, along with reports by other authors, was summarized at an ONR symposium (Ref. 6).

METHOD

FIELD WORK

Sources

A CW source at 162 dB re 1 μPa at 1 m emitting a 50-Hz sine wave was towed in a triangular pattern over the continental shelf area west of the NOSC tower in August, 1978 (Fig. 2). An additional 40-Hz tone of unknown source level was associated with the tow boat. In February, 1979, a 100-Hz CW source was towed in a circular pattern of 1-km radius about the receivers. These data were used to document the directionality gain of the geophones (Fig. 3).

In December, 1978, a shot run was made with the USNS DE STEIGUER from 1.4 mi (2.59 km) to a range of 43.8 miles (81.3 km) west of the tower (Fig. 4). The shots were made up of from one to four 1.8-lb MK 64-0 SUS charges set to explode at 60 ft (18.28 m) over the continental shelf, and 800 ft (243.84 m) in deeper water off the edge of the shelf. The "shallow" and "deep" shots were alternated over the last three-quarters of the run, the size of the deep shots being increased at the longer ranges. The shallow shots were fired with SUS launcher when a single 1.8-lb shot was detonated, while for a 3.6-lb "shallow" shot, one SUS charge was fired by launcher, and the other dropped over the side at the instant the first one hit the water. Charges of 3.6, 5.4, and 7.2 lb at 800 ft were made up of two, three, and four SUS charges taped together; details of the shot schedule are shown in Table 1. Shot instants were transmitted to the radio receiver in the tower by placing the microphone of the ship's laboratory radio set against the deck at the time the shock wave reached the ship. Radio reception was excellent throughout the shot run and the shot instants were well recorded at the tower.

Receivers

Two triaxial arrays of Walker-Hall-Sears, Inc., Model M-Z-3 geophones (N-S, E-W, and vertical) orthangonally mounted on an angle iron framework (Fig. 5) were buried about 6 in (15.24 cm) in the sand by the divers. The instruments were leveled by the use of a bubble level mounted atop the angle iron frame, and the N-S geophone was correctly

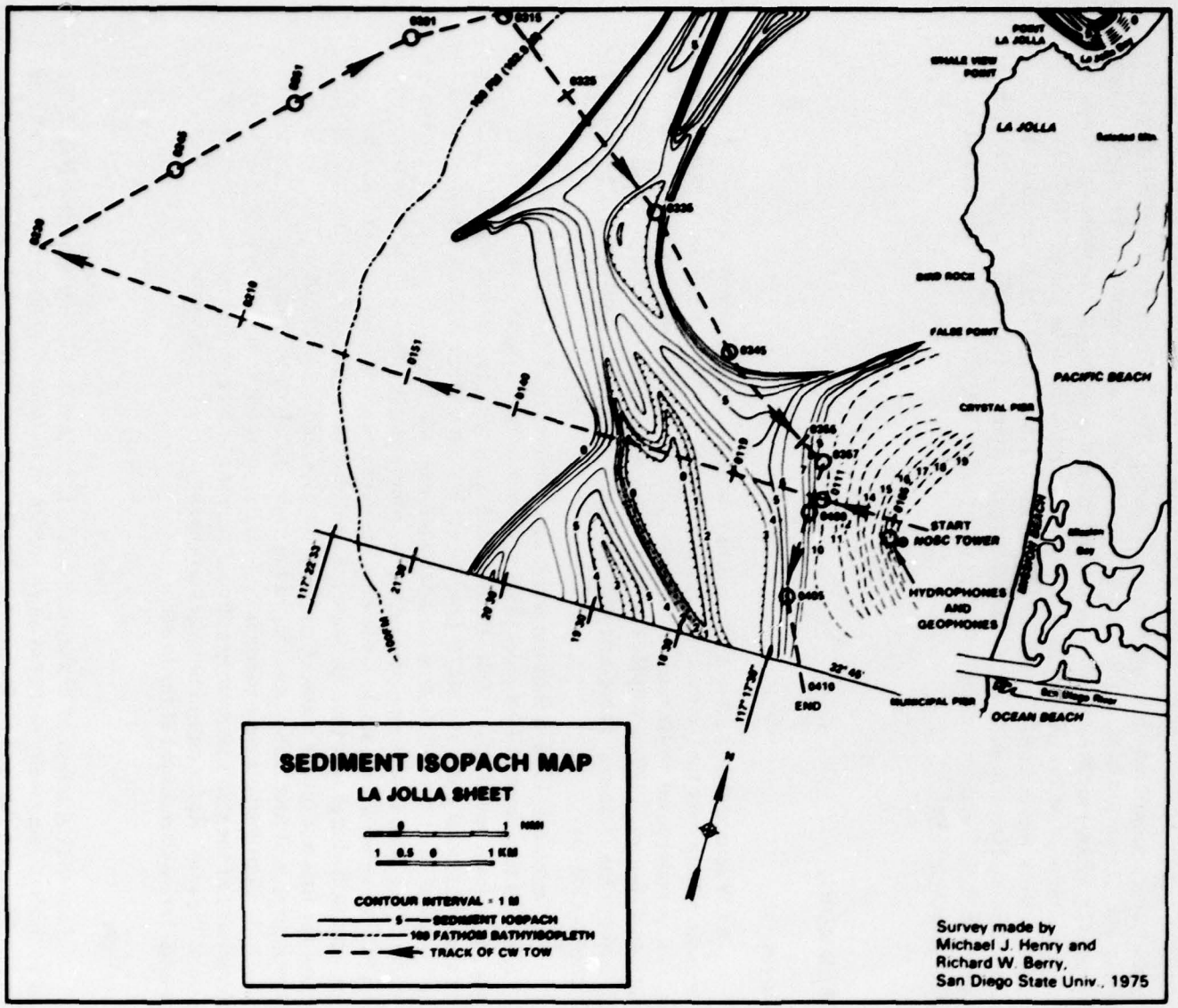

Figure 2. Chart of the NOSC tower area showing the track of the CW tows.

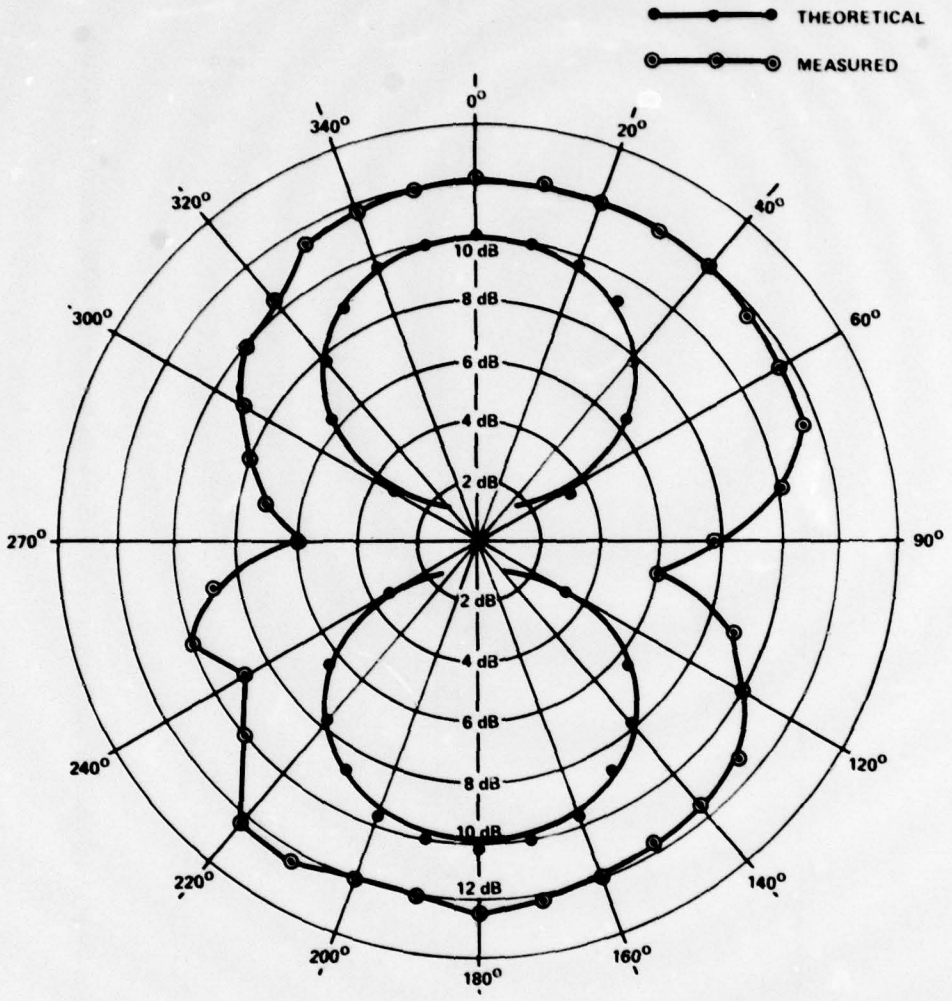

Figure 3. Directionality response of the N-S geophone compared to the theoretical response.

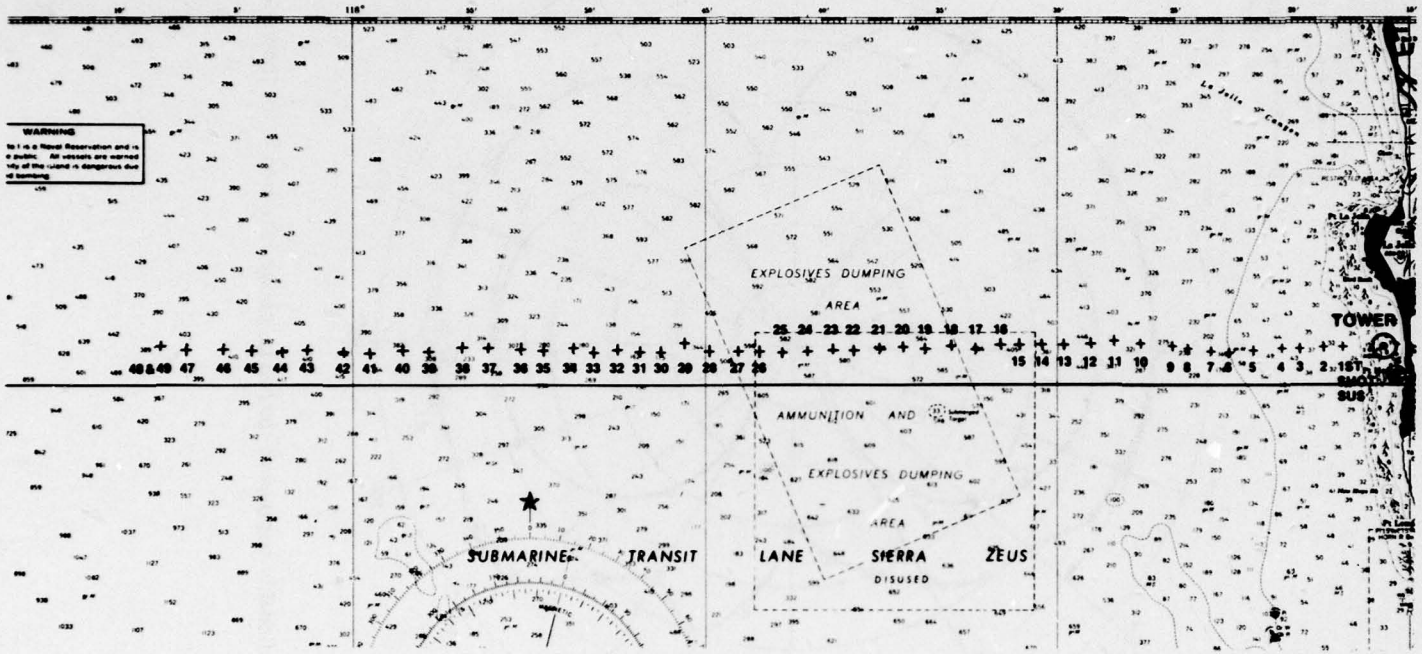

Figure 4. Chart of the San Diego trough showing the location of the SUS charges west of the NOSC oceanographic tower.

Table 1. Shot size, depth, range, and water depth beneath the ship.

SHOT	SIZE (lb)	DEPTH (ft)	RANGE (nmi)	RANGE (km)	WATER DEPTH (m)
TEST	1.8	60	1.4	2.58	43.8
1	1.8	60	1.45	2.68	47.5
2	1.8	60	2.15	3.98	54.8
3	1.8	60	2.95	5.46	64.0
4	1.8	60	3.65	6.75	73.1
5	1.8	60	4.7	8.7	84.1
6	1.8	60	5.6	10.37	122.5
7	1.8	60	6.25	11.57	374.9
8	1.8	60	7.05	13.05	418.8
9	1.8	60	7.9	14.63	484.6
10	1.8	60	8.75	16.2	537.6
11	3.6	60	9.5	17.59	610.8
12	3.6	60	10.5	19.44	749.8
13	3.6	60	11.4	21.1	850.3
14	3.6	60	12.2	22.59	731.5
15	3.6	800	13.1	24.26	694.9
16	3.6	60	13.93	25.8	819.3
17	5.4	800	14.57	27.0	974.7
18	3.6	60	15.5	28.7	976.5
19	5.4	800	16.8	31.1	987.5
20	3.6	60	17.54	32.5	1002.1
21	5.4	800	18.61	34.48	1011.3
22	3.6	60	19.35	35.85	929.0
23	7.2	800	20.50	37.97	1018.6
24	3.6	60	21.76	40.3	1031.4
25	7.2	800	22.0	40.76	1047.9
26	3.6	60	23.81	44.1	1064.3
27	7.2	800	24.1	44.64	1073.5
28	3.6	60	24.94	46.19	914.4
29	7.2	800	25.48	47.2	325.5
30	3.6	60	26.78	49.6	310.8
31	7.2	800	28.07	52.0	288.9
32	3.6	60	28.67	53.1	274.3
33	7.2	800	30.29	56.1	329.1
34	3.6	60	30.56	56.6	477.3
35	7.2	800	31.37	58.1	515.7
36	3.6	60	32.61	60.4	530.3
37	7.2	800	33.04	61.2	544.9
38	3.6	60	33.8	62.6	501.1
39	7.2	800	34.88	64.6	537.6
40	3.6	60	35.91	66.5	530.3
41	7.2	800	37.36	69.2	665.6
42	3.6	60	37.63	69.7	658.3
43	7.2	800	38.49	71.3	693.1
44	3.6	60	39.47	73.1	702.2
45	7.2	800	40.17	74.4	705.9
46	3.6	60	40.98	75.9	704.1

Table 1. (Continued)

SHOT	SIZE (lb)	DEPTH (ft)	RANGE (nmi)	RANGE (km)	WATER DEPTH (m)
47	7.2	800	41.74	77.3	715.1
48	1.8	60	42.65	79.0	727.8
49	3.6	60	43.89	81.3	731.5
50	5.4	800	43.89	81.3	731.5

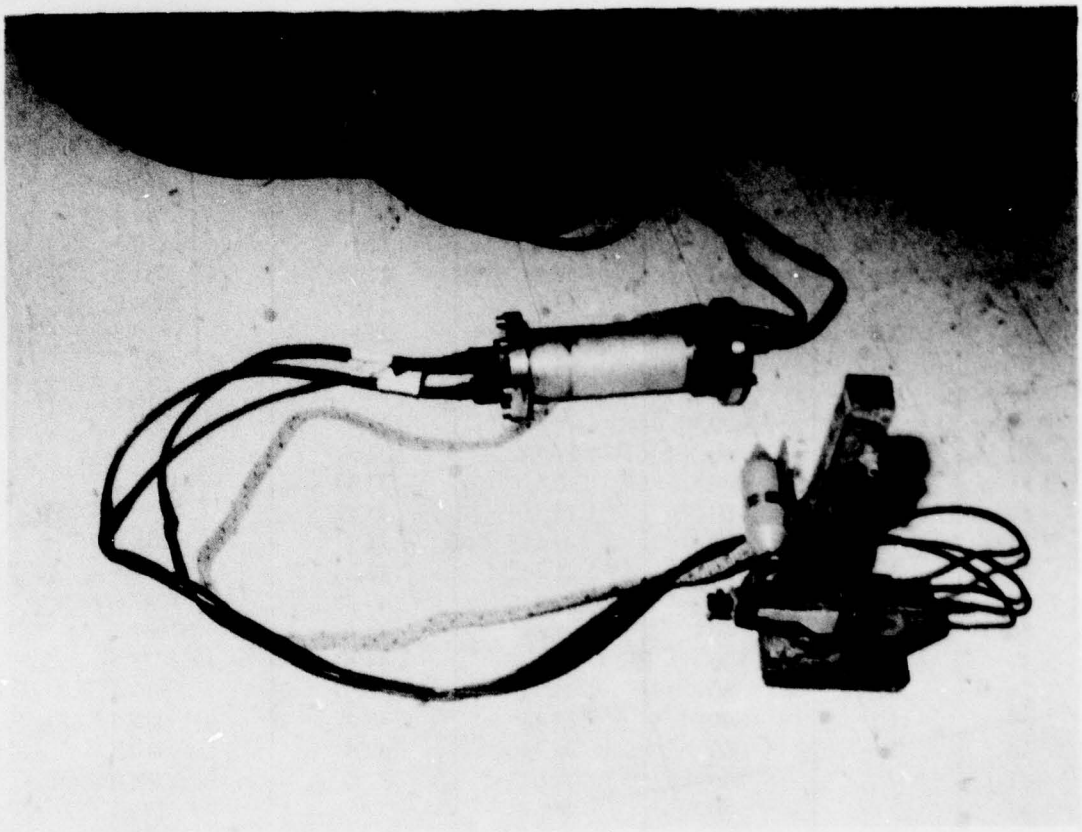

Figure 5. Photograph of the three-component geophone array that was used for detection of sound in the ground at the NOSC oceanographic tower.

oriented by the divers. An additional array of five E-W oriented geophones was deployed at 1,000 ft (304.8 m) bearing 045 deg. (T) from the tower for the August exercise. The geophones had a sensitivity of about -124 dB re 1 μPa and a natural frequency of 8 Hz. Figure 6 shows the frequency response curves for the geophones.

Two hydrophones were deployed at each of the geophone clusters, one on the bottom and one buried about 9 in (22.86 cm) in the sediment. These hydrophones were of the pressure-sensitive ceramic type and had sensitivity of about -110 dB re 1 μPa. They had a flat response down to about 20 Hz with a roll-off of about 8 dB per octave below that (Fig. 7). For the shot run, a relatively insensitive hydrophone was suspended from the tower

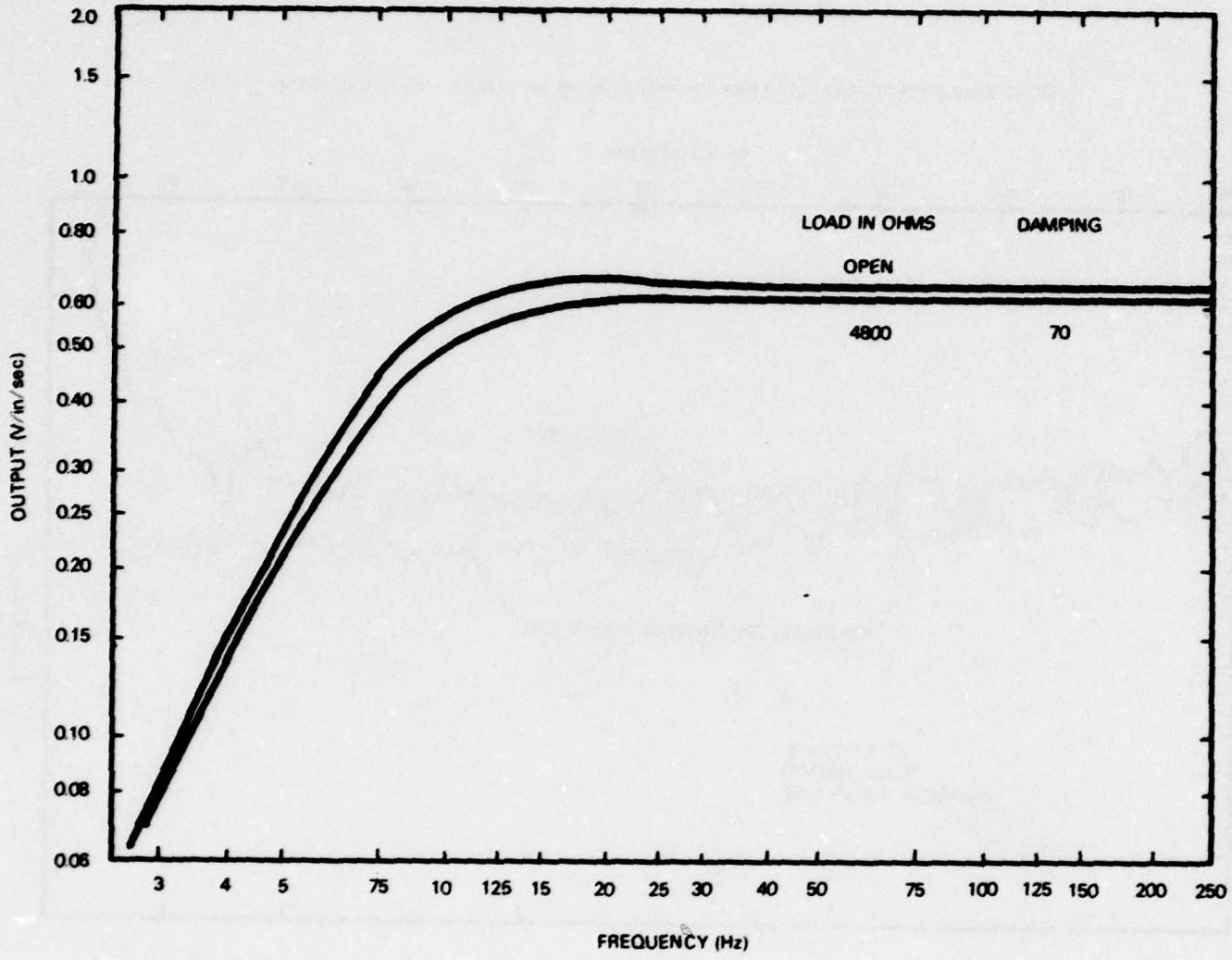

Figure 6. Frequency response curve for the Walker-Hall-Sears Model M-Z-3 geophones used in the experiment.

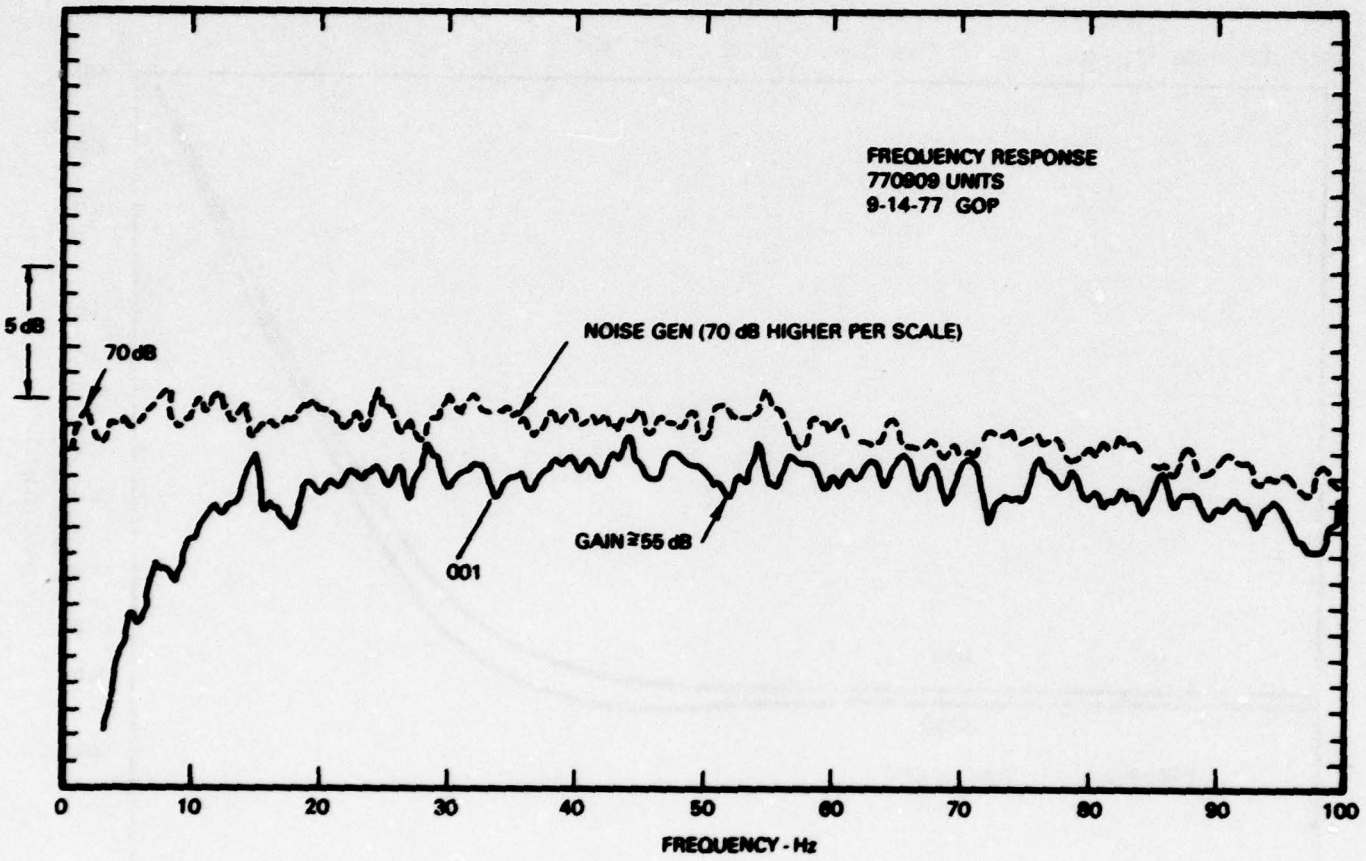

Figure 7. Frequency response curve for the hydrophones used in the experimental work at sea.

for recording high-level shot signals from close-in shots causing overloading of the other detectors. At the time of the shot run, this insensitive hydrophone became inoperative (apparently due to leakage), one of the vertical geophones was also inoperative, and one of the E-W geophones appeared to give peculiar results. Later analysis of the records showed that the response of this E-W unit was intermittently saturated at 44 and 88 Hz, a condition believed due to tilt (the horizontal geophones have to be within 3 deg of horizontal to function properly). Therefore data from this geophone and its orthagonal N-S unit were not used in the results (the vertical geophones are not nearly as sensitive to leveling as the horizontal units). Data were recorded on a 14-channel AMPEX 1300A FM magnetic tape recorder for later processing and a 12-channel model 906C Honeywell Visicorder for visual monitoring of the shot signals.

Analysis

The tape recordings were played back on the same unit that recorded them, using the same amplifiers (Ithaco Model P11) used in the field. Narrowband frequency analysis of the signals was done on a Spectrum Dynamics Model 330 spectrum analyzer and displayed on a Hewlett Packard Model 7035B X-Y plotter (Fig. 8). For analysis of the shot records, the SD-330 analyzer was operated in two modes: transient capture and peak hold (Fig. 9). The CW signals were analyzed in the eight-pulse averaging mode and displayed on a Moseley Model 680 Autograf recorder (Fig. 10). The Visicorder was used in analysis for display of sections of the recordings requiring more detail than was available on the records made in the field. Source levels for the SUS charges were computed from Ref. 8.

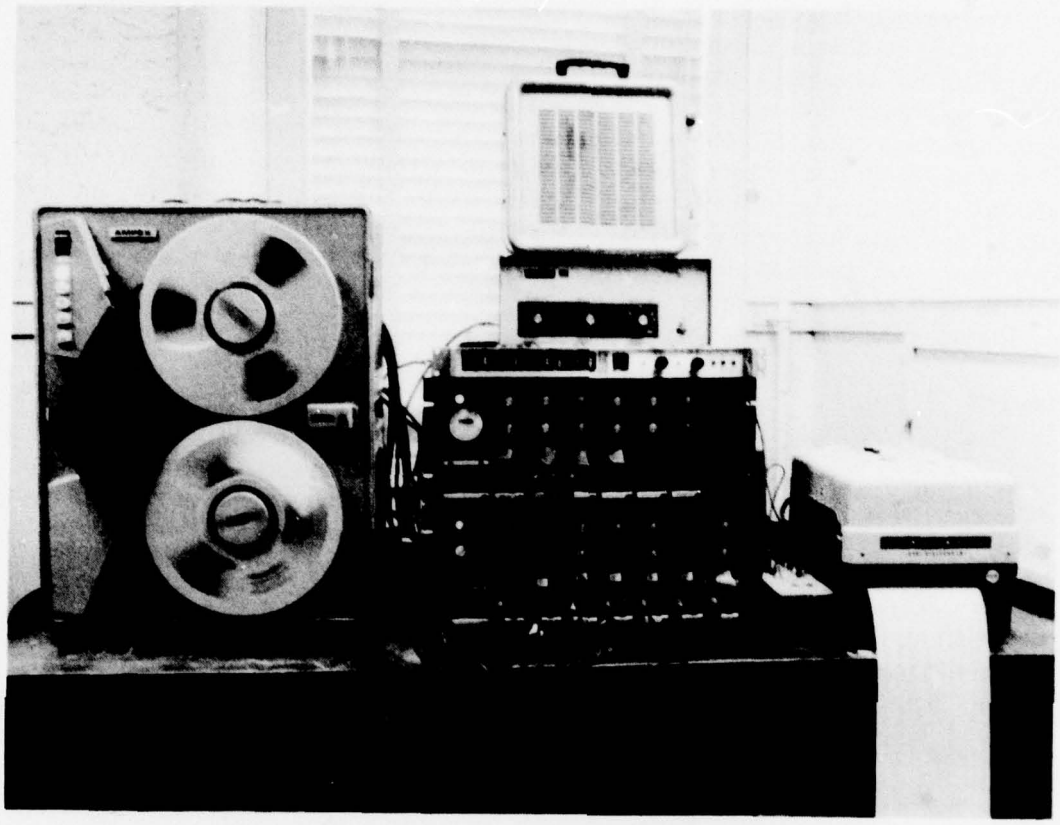

Figure 8. Photograph of the recording/analysis equipment used in the experiment.

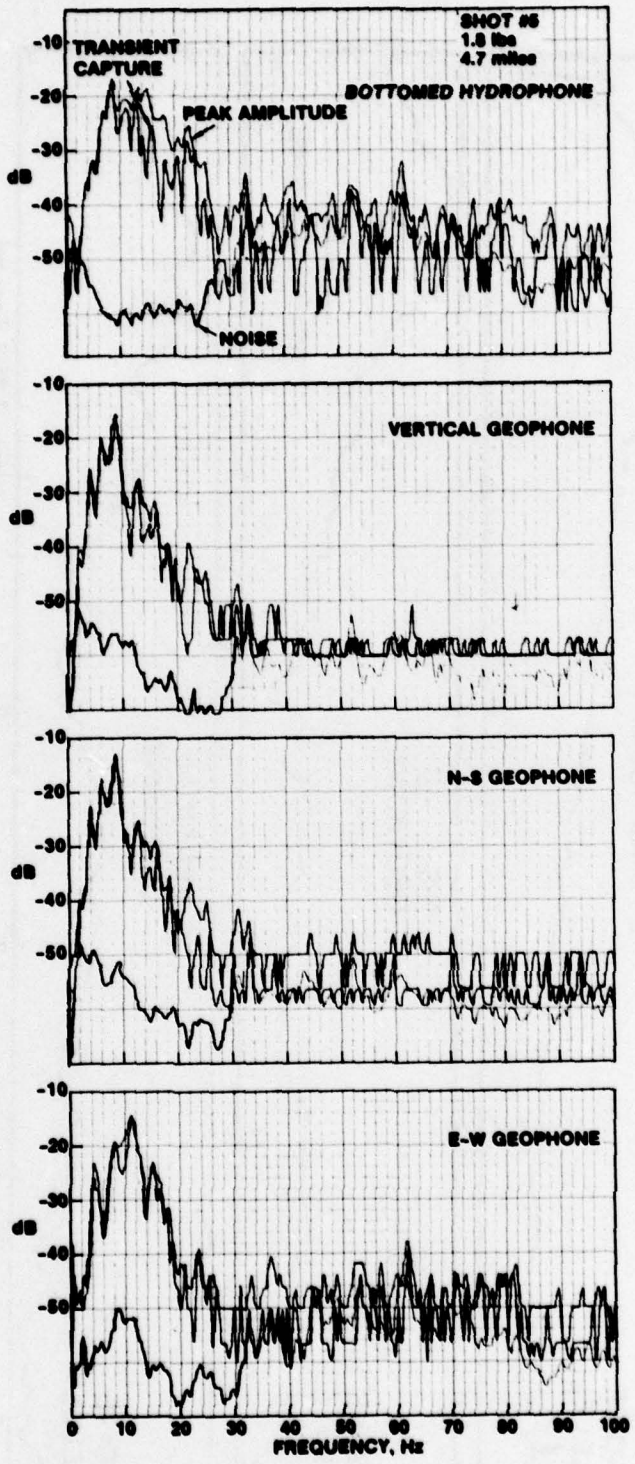

Figure 9. Frequency spectrum analyses of signals from a 1.8-lb "shallow" shot at 4.7 miles (8.7 km) showing both the transient capture and peak hold results.

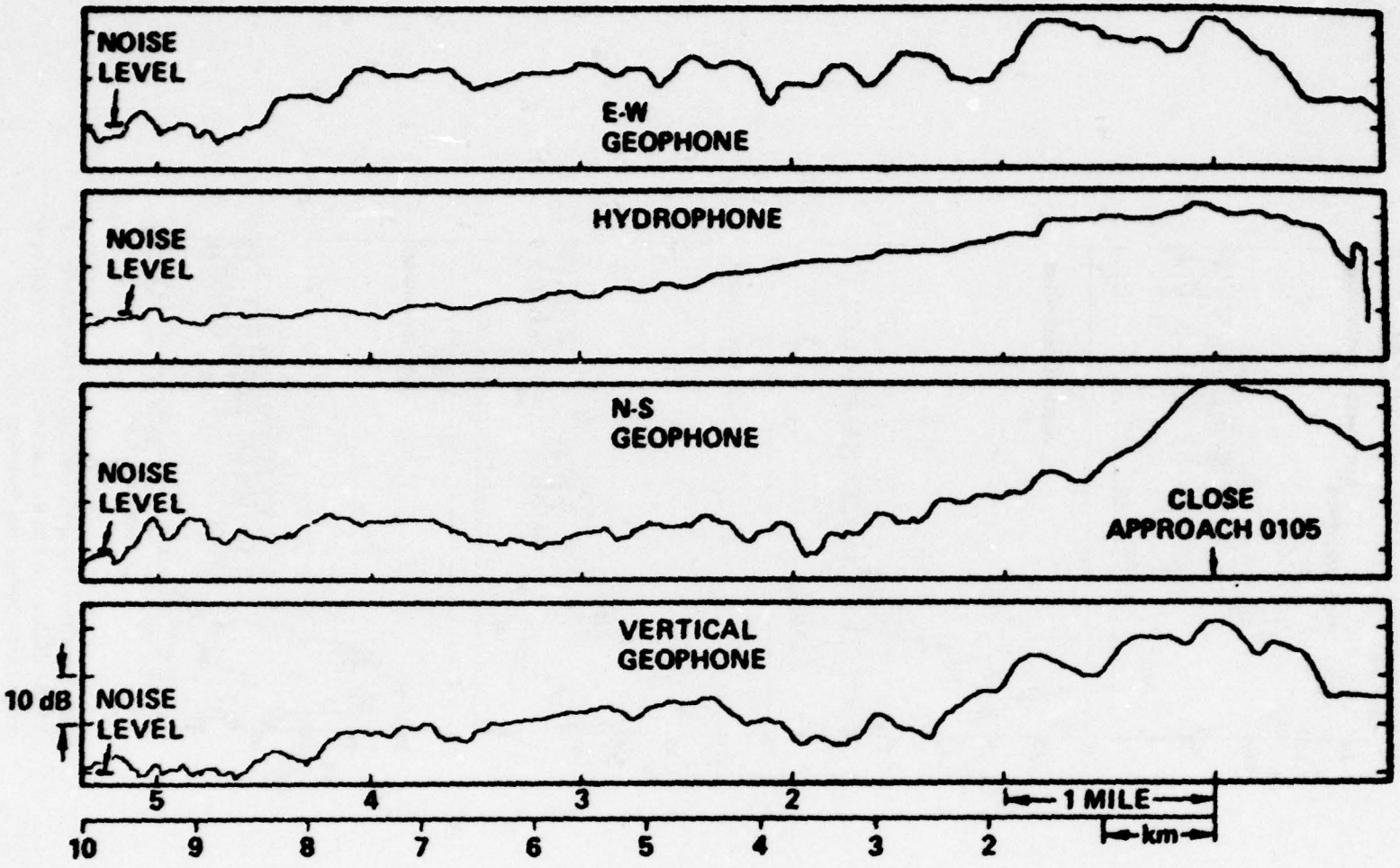

Figure 10. Playback of the signal level vs time recording for the 40-Hz CW signal as recorded on the E-W geophone. Null at CPA, caused by the transmitter being north of the detector, is about 7 dB, which indicates the directionality gain of this geophone.

RESULTS

PROPAGATION

General

Propagation was by SR/BR (Surface Reflected/Bottom Reflected) ray paths for both the deep and shallow shots. As shown in Fig. 11, the sound rays were concentrated both over Thirtymile Bank and the continental shelf. Some additional rays were reflected from the flanks of Thirtymile Bank and show up as later arrivals of shots 13 through 27. Computed propagation loss is marked by the lack of convergence zone peaks and an 8- to 10-dB up-slope enhancement (Fig. 12).

Measured propagation loss for the 40-Hz and 50-Hz CW runs over the continental shelf section is known in somewhat better detail. The 40-Hz data show various peaks and troughs associated with cancellation and reinforcement of propagation modes to be more prominent in the E-W and vertical geophone data than the N-S geophone and hydrophone data (Fig. 13). Also, as shown in the figure, propagation loss is greater over the area of thickening, unconsolidated sediment than where there are rock outcrops, and the E-W geophone was the only one that received data at ranges beyond the sedimentary basin.

The 50-Hz data were reduced to spectrum levels so that the CW and shot levels could be plotted on the same scale (Fig. 14). As shown in the figure, the vertical geophone data again show prominent mode interference patterns, whereas the E-W, N-S, and hydrophone data do not. At longer ranges, the shot data show mode interference peaks of about 5–6 dB for all the detectors. No one unit appears to be superior throughout, but the hydrophone data show greater loss than the geophone data in the range interval 7–18 km. The overall loss appears to be about 20 Log R_1 + 10 Log R_2, where R_1 is 300 m (the point of closest approach of the CW tow to the detectors) as shown by the dashed curve in the figure.

No close-in data were available for frequencies below 40 Hz because the first three SUS charges overloaded all the detection systems. Data from shots 4 through 11 (at ranges of 6.75 to 17.59 km) are shown in Figs. 15a-15d for frequencies of 5, 10, 20 and 30 Hz, respectively. As shown in the figures, the geophones showed less loss than the hydrophone, except at 20 Hz, where the hydrophone performed as well or better than the geophones. (This effect may be produced by the roll-off of the hydrophone's response, which is sharper than that of the geophone.) Even so, the 30-Hz data show the hydrophone loss to be greater than the geophone's, and at this frequency, both types of detectors have a flat response.

Beyond the edge of the shelf (shot 11) no obvious ground arrivals were noted on the records. For shots at greater ranges, the S/N of the hydrophones was greater than of the geophones for frequencies above 5 Hz. Examples of these data are shown in Figs. 16a-16d, for shots 32, 36, 46, 49, and 50 for frequencies of 5, 10, 20, 30, 40, and 50 Hz, respectively. Figure 17 shows the type of spectral analysis from which these data were measured.

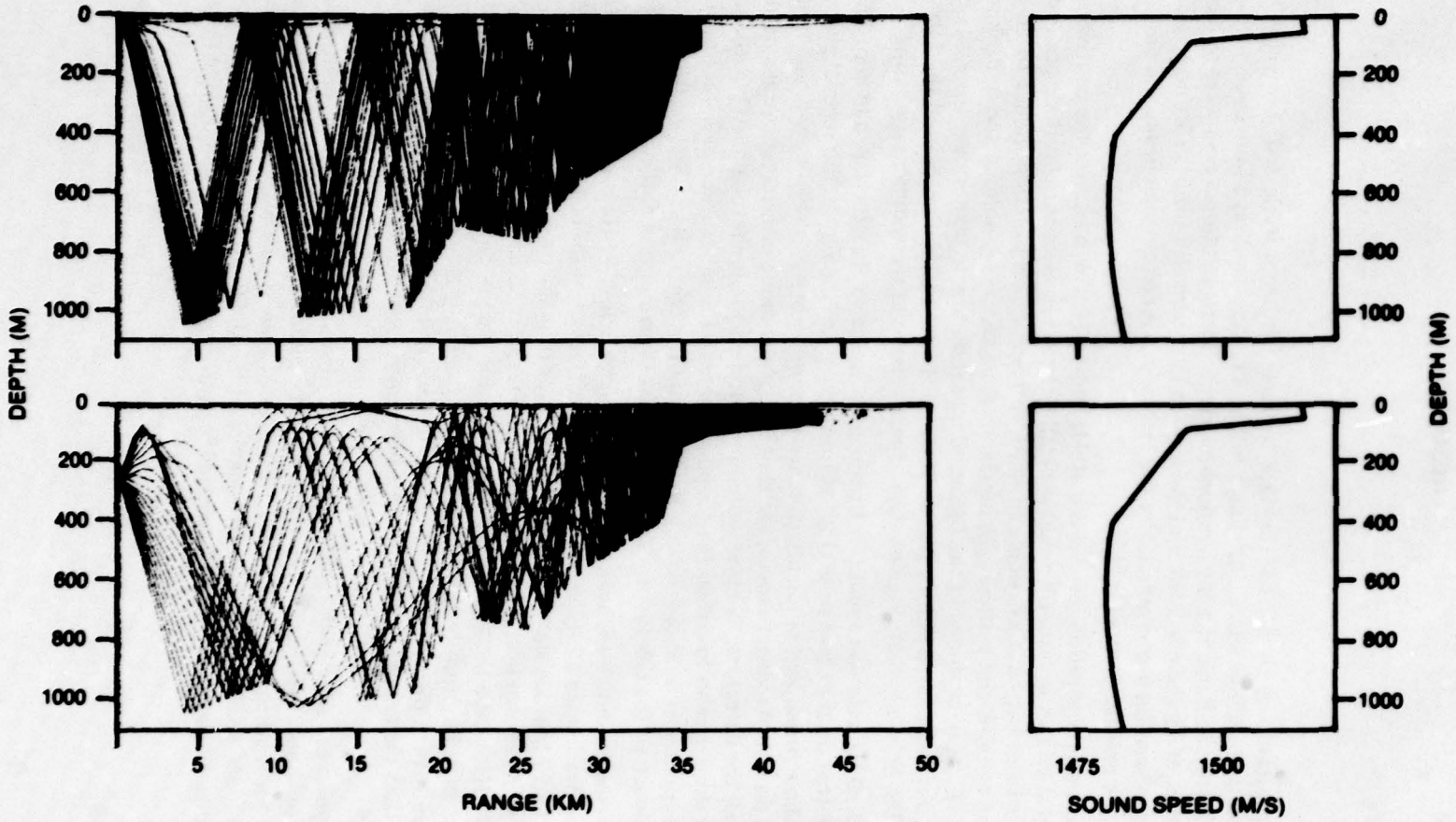

Figure 11. Sound ray tracing for the "deep" and "shallow" shots. Rays traced are from -16 to +16 deg in 1-deg increments.

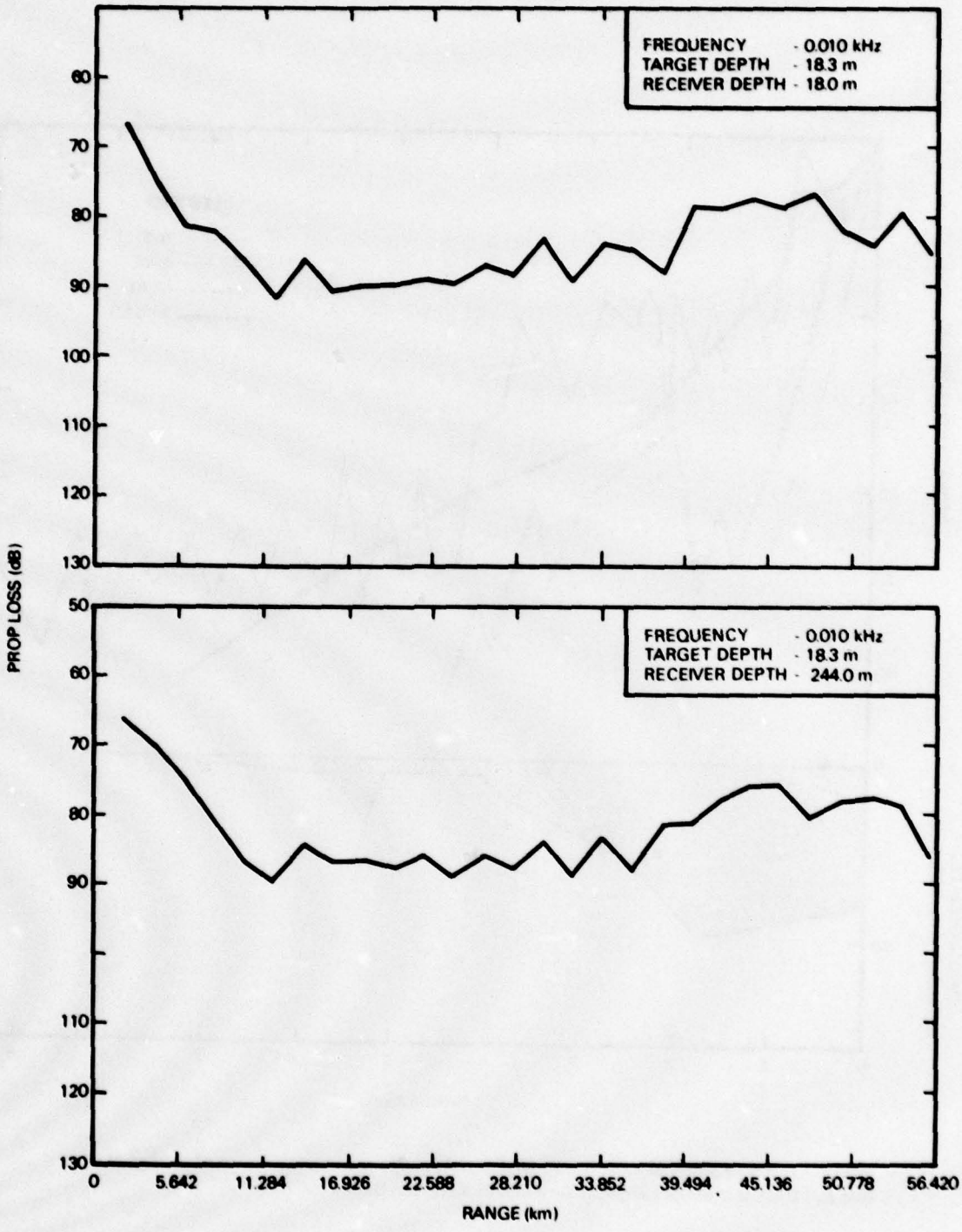

Figure 12. Propagation loss curves, computed using the RAYWAVE method (Ref. 9) for the "deep" and "shallow" shots.

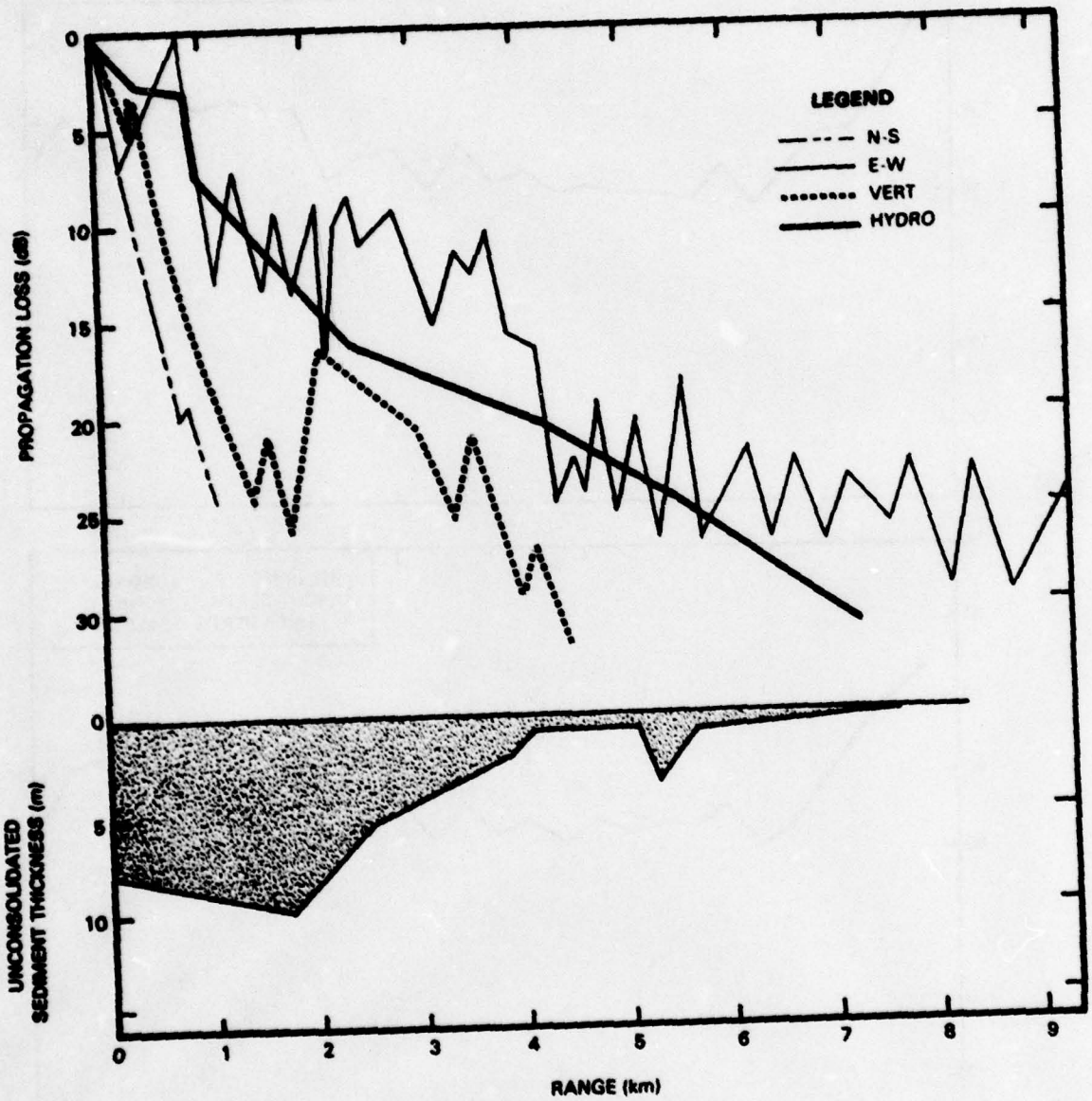

Figure 13. Propagation loss for the 40-Hz CW data showing the relationship of propagation loss and thickness of unconsolidated sediment along the track.

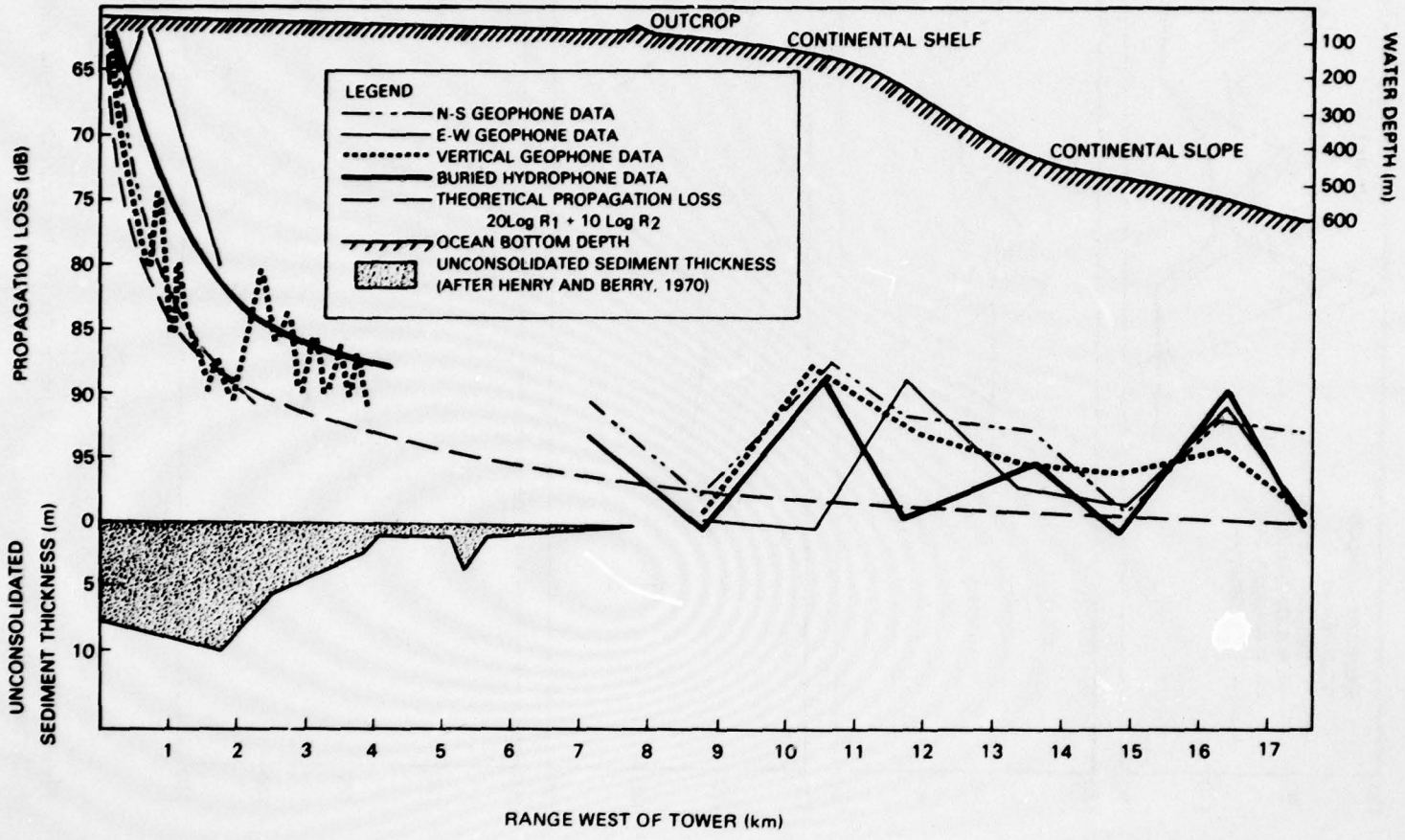

Figure 14. Propagation loss of the CW and shot data for 50 Hz out to the edge of the continental shelf. Dashed line shows computed propagation loss.

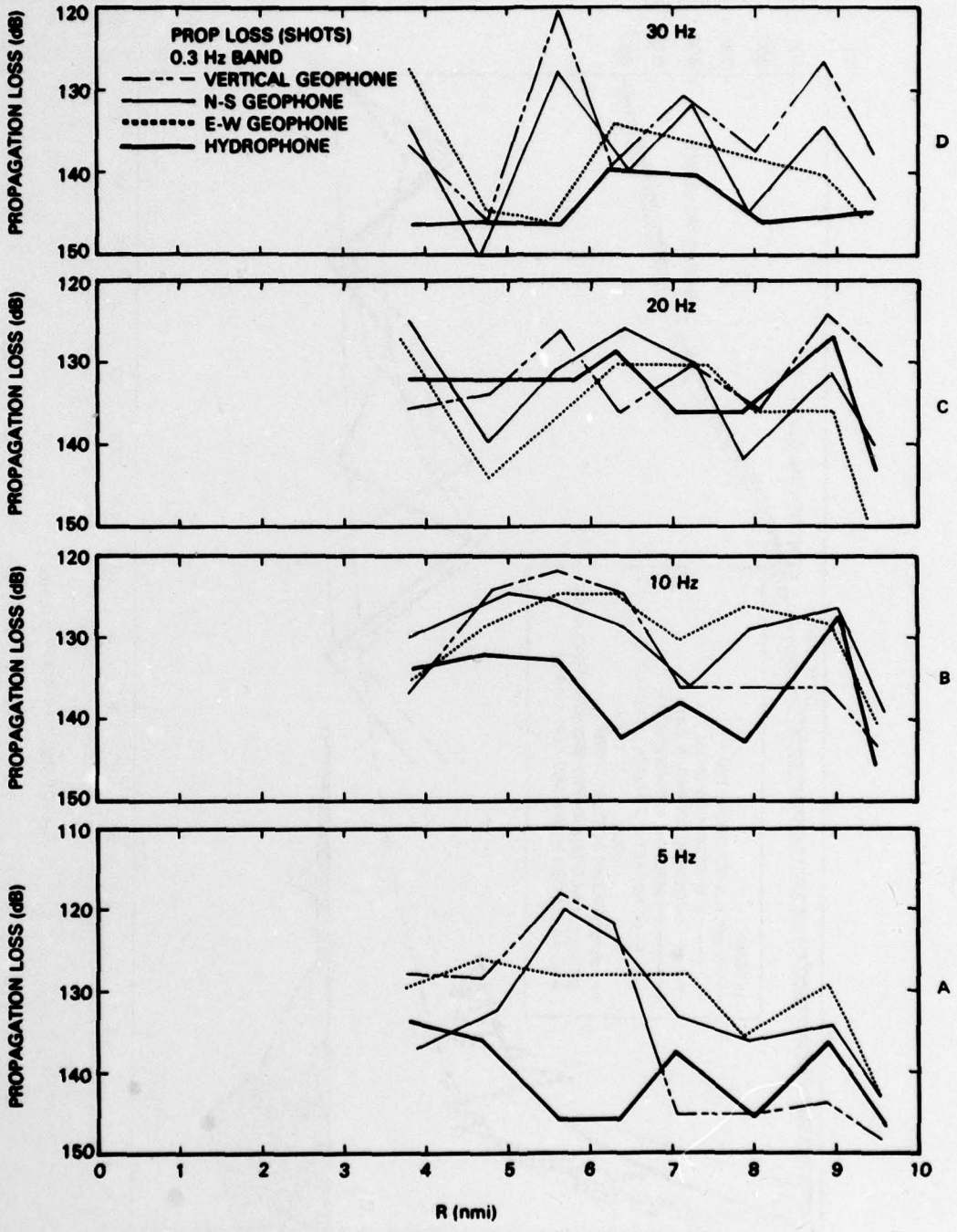

Figure 15. Propagation loss (at indicated frequencies) for the hydrophone and geophones in the tests with explosive sources.

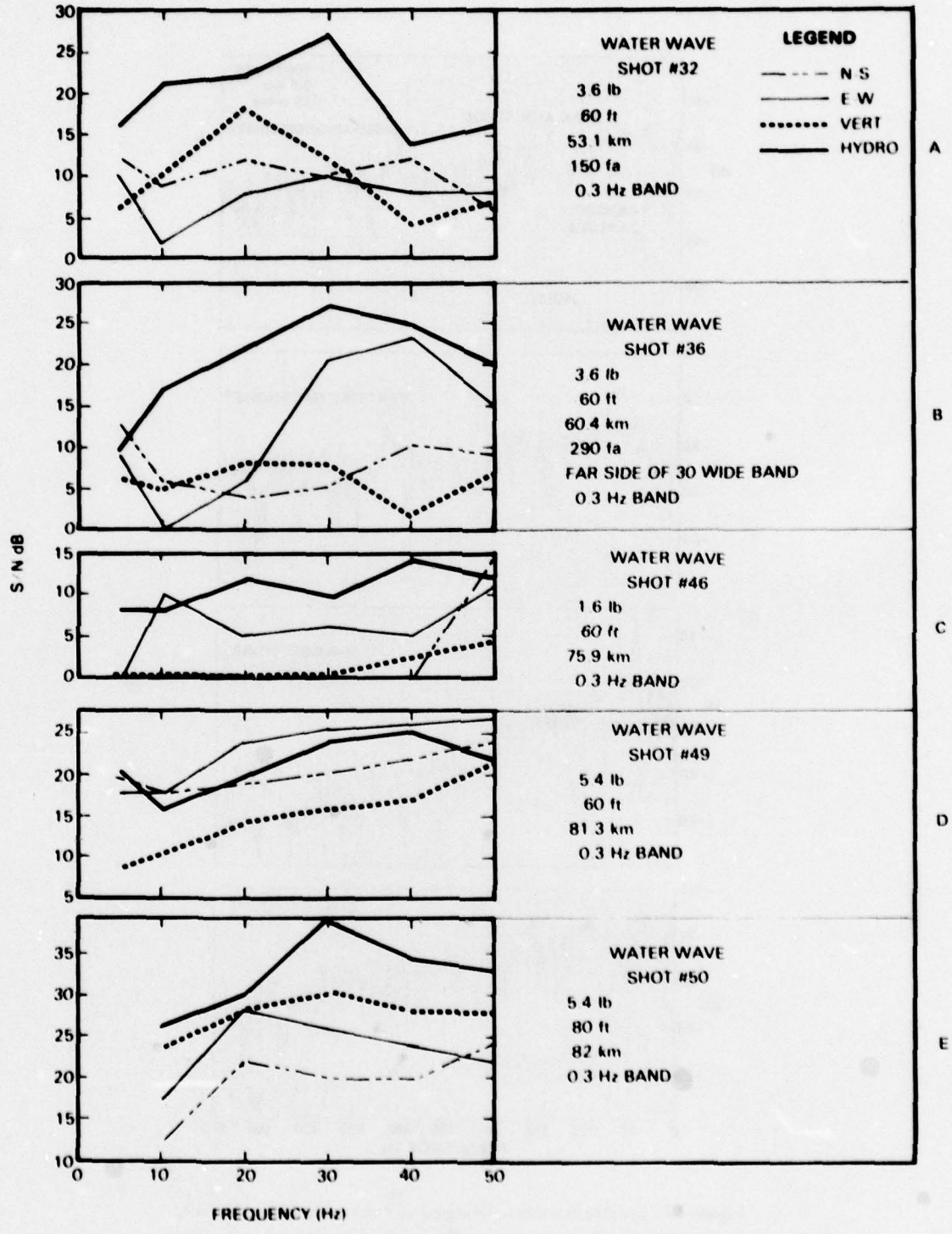

Figure 16. Hydrophone and geophone signal-to-noise ratios for frequencies below 50 Hz (explosive sources).

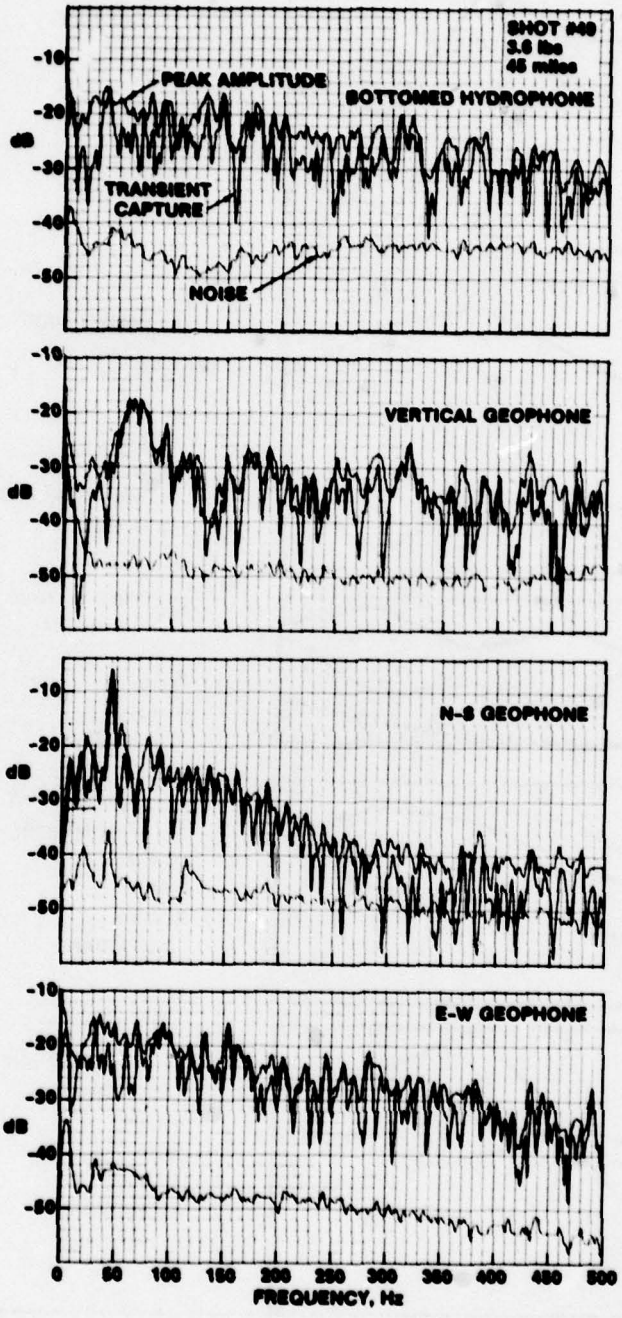

Figure 17. Spectrum analysis of signal and noise levels for shot 49, the last "shallow" shot in the profile in a 3-Hz bandwidth for frequencies up to 500 Hz.

Ground Arrivals

Shots 1-11 over the continental shelf and slope showed prominent ground arrivals preceding the water arrival. As shown in Fig.18, the arrivals appear on both the hydrophone and geophone traces. The first arrival shown in the figure is the arrival of the compressional or (P) wave through the ground; the next (in time) prominent arrival is interpreted as a shear or (S) wave; and the last, and most intense, arrival is the water wave, i.e., energy that traveled with the speed of sound in water between source and receiver.

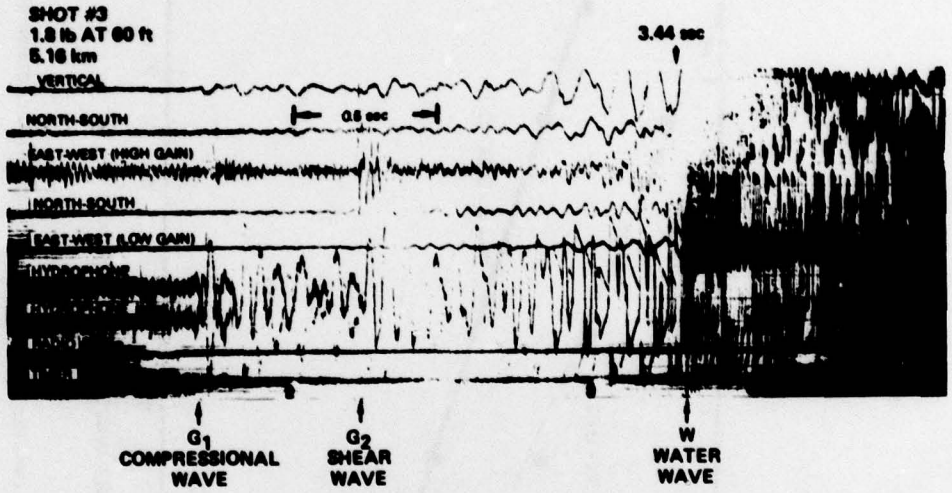

Figure 18. Oscillograph recording of shot 3 showing the hydrophone, geophone, and radio signals received. Note the prominent S (shear) wave arrival after the initial P (compressional) wave arrival.

Based on these arrival time data, a plot of water wave travel time vs ground wave travel time was constructed (Fig. 19). As shown in the figure, the P arrivals form a straight line having an intercept of 0.7 s, and a slope of about 3.2 times that of the water wave (which has a slope of 1). With this information, the thickness and sound speed of the refracting layer can be determined by means of the standard formulas for refraction profiling calculation (see for example Ref. 10):

$$Z = \frac{t_i}{2} \frac{V_2 \times V_1}{\sqrt{V_2^2 - V_1^2}} \qquad (1)$$

where Z is the depth of the refracting layer, V_1 is the sound speed of the first layer, V_2 is the sound speed of the refracting layer, and t_i is the intercept. Since V_1 is known (Ref. 7) and V_2 can be determined from Fig. 19, the depth can be easily calculated to be 553 m.

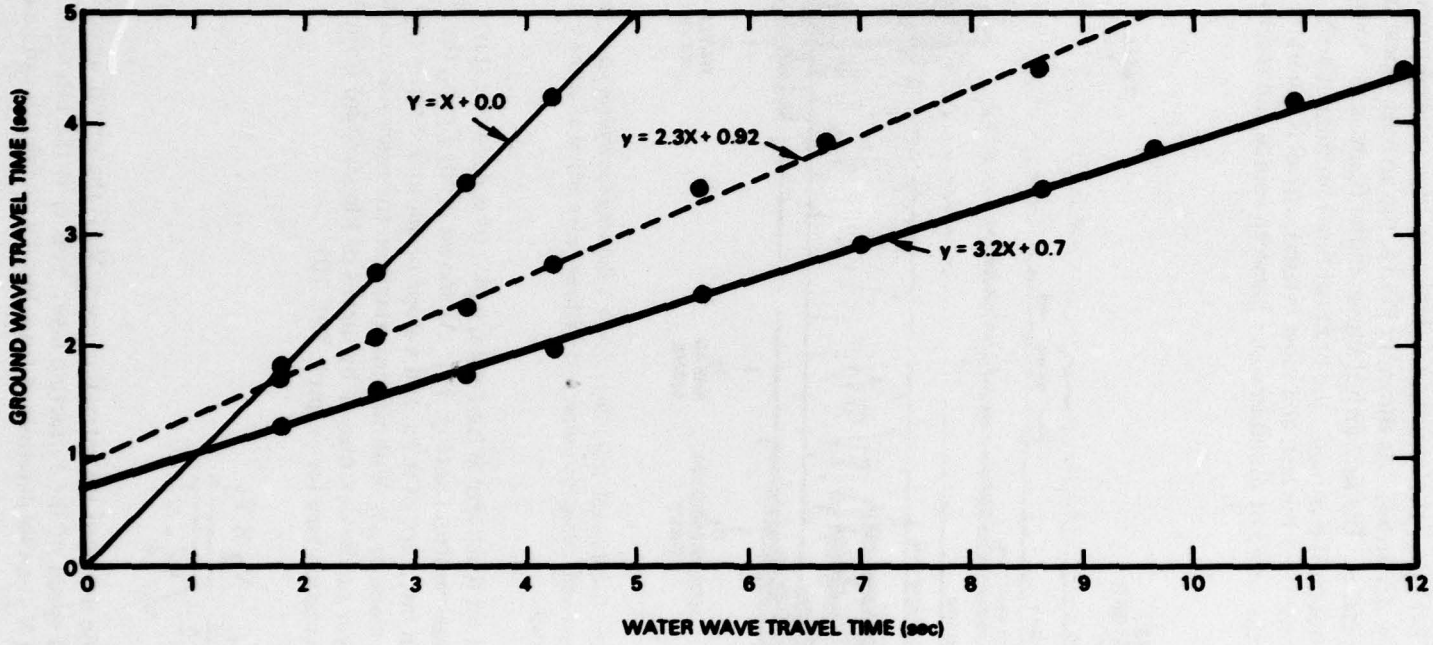

Figure 19. Travel time plot of the arrivals from shots over the continental slope, straight lines drawn by eye fit through the data points represent the best fit for the interpretation made in this report.

An additional line, shown in Fig. 19, having and intercept of 0.92 s and a slope of 2.3 times W, is based on secondary arrivals (as that marked G2 on Fig. 18). The arrivals determining this line are interpreted as being shear arrivals and give a sound speed of 3420 m/s which is close to that predicted (3038 m/s) for layer 5 (Ref. 7) and gives a V_p/V_s ratio of 1.71, which is near that expected with a Poisson ratio of 0.25. This interpretation requires that the energy was propagated as compressional waves in the water and sedimentary layers above the basement and converted into a shear wave at the consolidated sediment-basement interface (Ref. 11). The intercept value of 0.92 s supports such an interpretation because it gives a two-way travel time thickness of 2194 m, which is within 10 percent of that measured (Table 1). The S/N ratio of this second arrival (at $16^h\ 45^m\ 32^s$) is greater than for the first arrivals (at $16^h\ 45^m\ 29.5^s$) on all the detectors (Fig. 20) for shot 6, as is true for the other shallow-water shot data. This observation supports the interpretation of a shear-wave in the basement being converted to a P wave in the upper layers as described in Ref. 12. This type of "converted" P wave is believed to be due to a transformation of part of the compressional waves into vertically polarized shear waves (SV) at the contact between the sediment and the underlying crystalline rock, where nearly all of the energy is in the form of shear wave (Ref. 2)

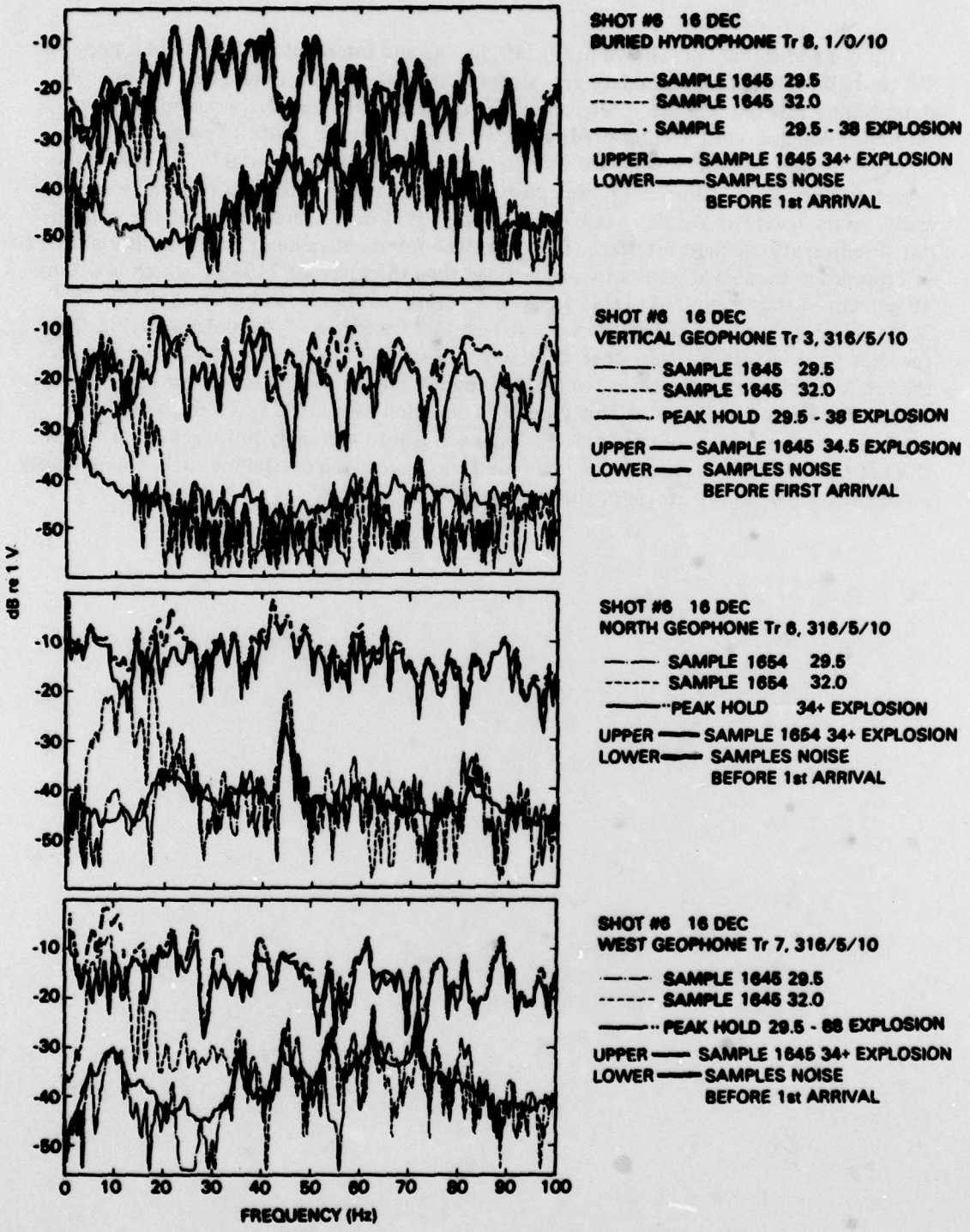

Figure 20. Spectrum analysis of the early ($16^h\ 45^m\ 29.5^s$) P arrivals, later S arrivals ($16^h\ 45^m\ 32^s$), and ambient noise for arrival time of shot 6 in the frequency band 0-100 Hz for both hydrophone and geophone data.

AMBIENT NOISE

Ambient noise during the summer (August) experiment was dominated by a strong cyclic component, thought to be due to an as yet unidentified biologic source (Ref. 13). These sounds, which have previously been described as of the "chorus-type" (Ref. 14), peak periodically at about 400 Hz, with amplitudes diminishing rapidly below 100 Hz and above 1000 Hz. The periodicity is typically about 45 s and amplitudes vary from barely discernible to 26 dB (Fig. 21). As shown in the figure, the troughs between peaks in the cycling sounds deepened near morning twilight and the time interval between peaks increased. The sounds were damped when local cloud cover occurred at 0630. Noise levels from this source were higher on the hydrophone recordings than on the geophone recordings and slightly higher on the E-W oriented geophone than on either the vertical or N-S geophone.

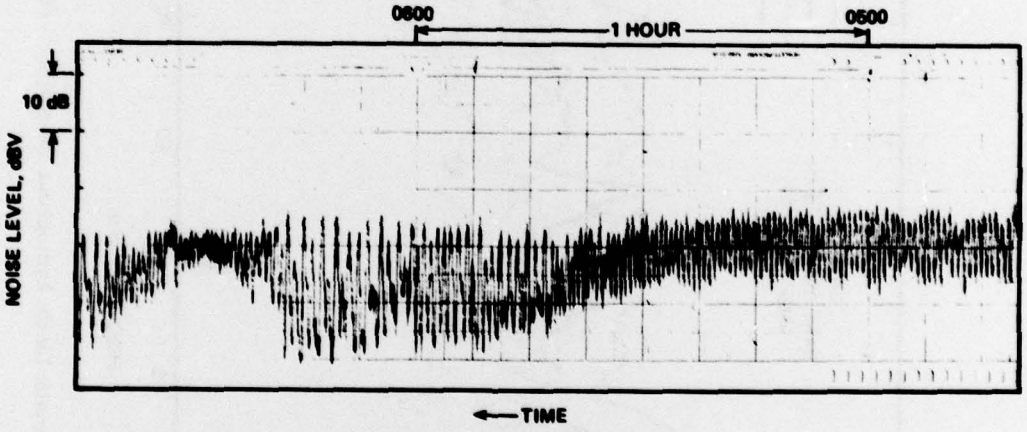

Figure 21. Ambient noise record for 24 August 1978, as detected on a bottomed hydrophone, in the 0- to 500-Hz band (3-Hz bandwidth).

The cyclic noise so prominent in summer appears to be absent in winter. The noise levels during the shot run (in December) were thus dominated by fishing vessels and surf. A typical example (Fig. 22) shows the noise level on the E-W geophone to be the highest in the 0- to 100-Hz band, the vertical geophone being next (below 50 Hz), the N-S geophone lower yet, and the buried hydrophone the lowest of all. (Generally, the buried hydrophone had a slightly lower noise level – and correspondingly better S/N ratio – than the bottom hydrophone.) The increase in noise level in the 30- to 70-Hz band, with some tonals near 30 Hz, was due to a ship that later passed fairly close to the tower. A strong (about 6-ft, as measured on the ladder at the tower) swell was running at the time, a light rain was falling, and there was a light wind from the SW. Surf along the beach (1.4 km to the east of the tower) was high, as it had been all day.

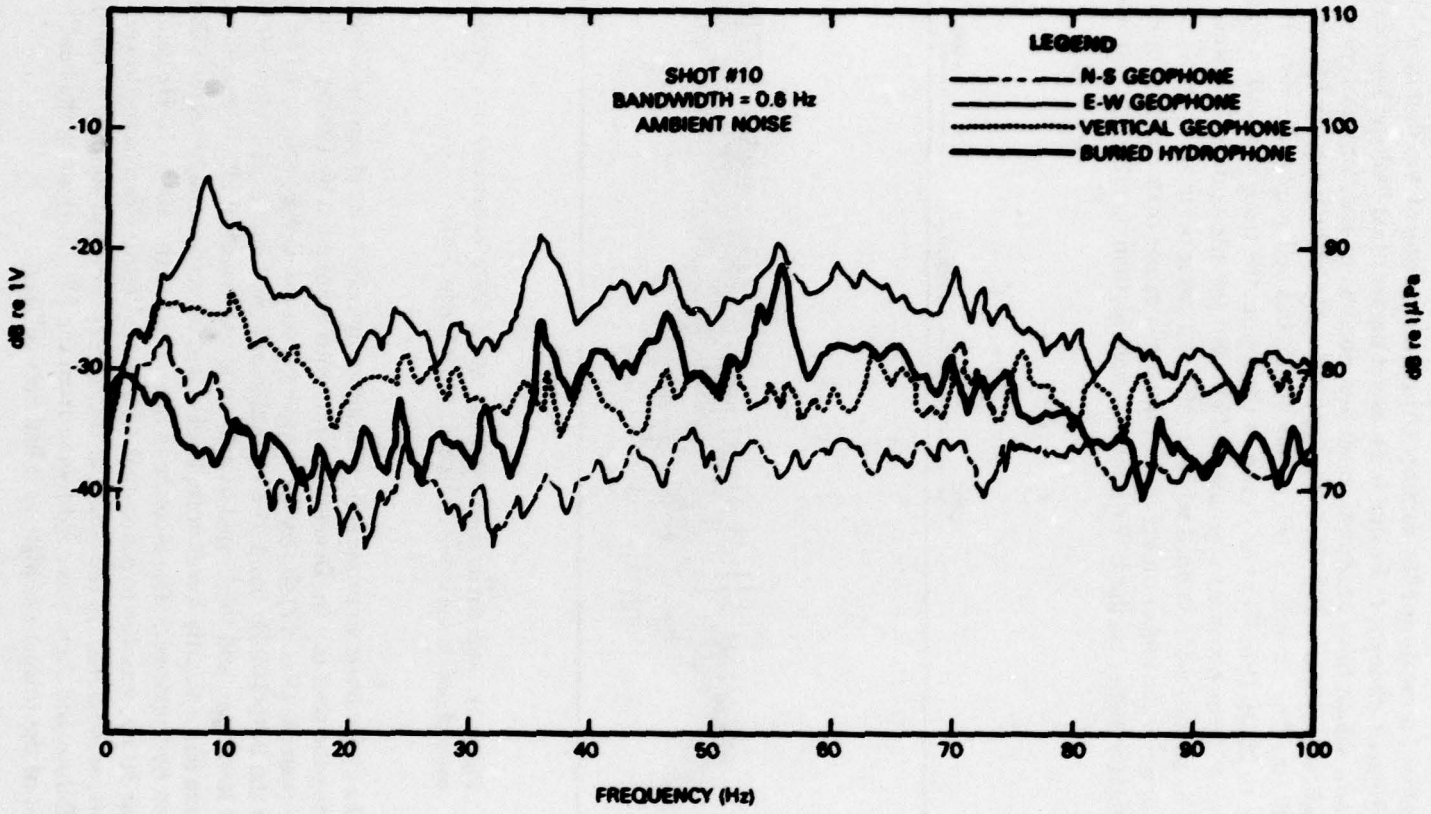

Figure 22. Ambient noise levels in the winter for the hydrophone and geophone detectors in the 0- to 100-Hz band.

GEOACOUSTIC MODEL

The geoacoustic model for the tower site consists of five layers. In descending order, with their corresponding compressional sound speeds, these are:

Water	1500 m/s
Unconsolidated	1798 m/s
Semiconsolidated	1855 m/s
Consolidated	4770 m/s
Basement	5860 m/s

Further details are shown in Table 2.

Table 2. Geoacoustic parameters of the NOSC tower area.

LAYER DESCRIPTION	VELOCITY (m/s) V_p	V_s	ATTENUATION CONSTANT (K)[a] K_p	K_s	DENSITY (gm/cm^3)	THICKNESS (m)	DEPTH (m)
1. Water	1499	–	–	–	1.025		
	1501	–	–	–		18.3	18.3
2. Unconsolidated (sand)	1798[b]	197[b]	0.4[b]	13.2	2.01[b]	8.2	26.5
3. Semiconsolidated (sand)	1855	331	0.3	13.2	2.14[c]		
	1875	396	0.3	13.2	2.14[c]		
	1917	482	0.2	4.8	2.0[3]	11.0	37.5
4. Consolidated (sandstone)	4770[d]	2783	0.1	3.4	2.6		
	4889	2794					
	4908	2805				553	590
5. Basement (basalt)	5860[e]	3420	0.03	0.07	2.83	1400	1990

(a) As in atten (dB/m) = Kf (kHz)

(b) In Situ measurement by divers (Ref. 15)

(c) Well log data

(d) Apparent velocity

(e) Seismic refraction measurement

These parameters were input data for an FFP (Fast Field Program) computer model (Ref. 16) for calculating propagation loss. The program takes into account both the compressional and shear wave velocity and attenuation in the sediments as well as the density and thickness of layers. Comparison of the calculated and observed loss at 50 Hz is quite good, as shown in Fig. 23. The program has an option for calculating the ground motions in millimicrons for the north-south, east-west, and vertical geophones.

Seismic Gain

The term "sesmic gain" as used by Urick (Ref. 1) describes the difference in S/N observed on geophone records compared to that observed concurrently on geophone records. For the close-in shots (less than 5 km), seismic gain of 5–8 dB is computed from the data of Fig. 9. As shown in Fig. 24, there is 4–8 dB seismic gain at 5 and 15 Hz for the vertical and E-W geophones, but only at 5-Hz for the N-S geophone.

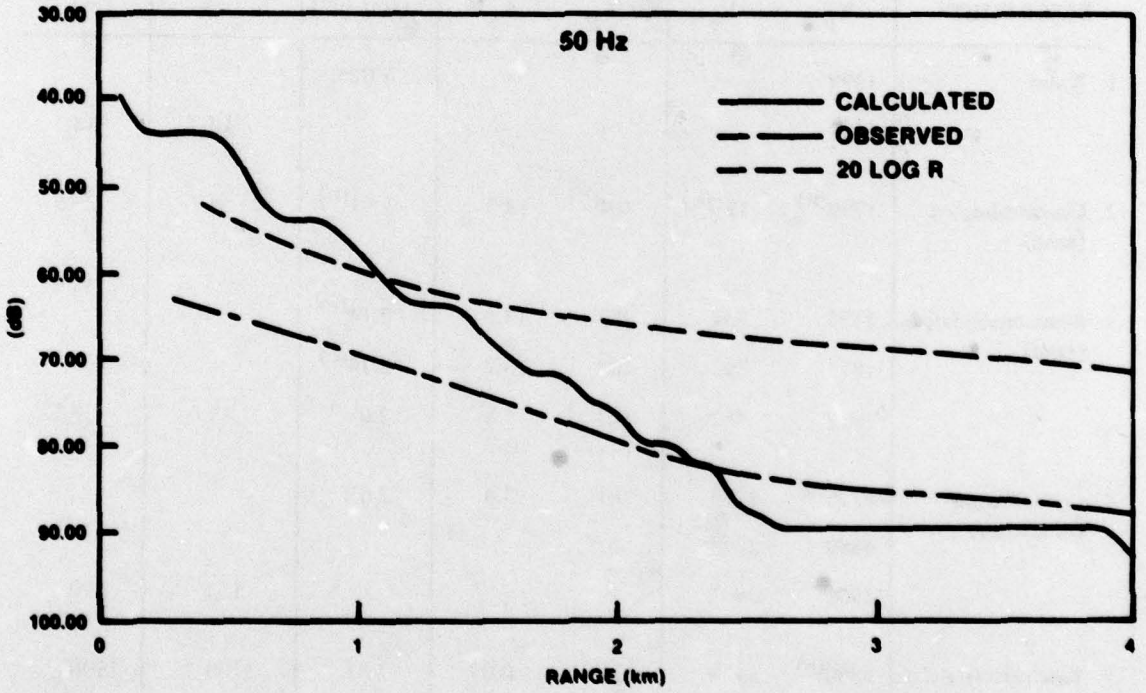

Figure 23. Computed and observed propagation loss to 50-Hz hydrophone data.

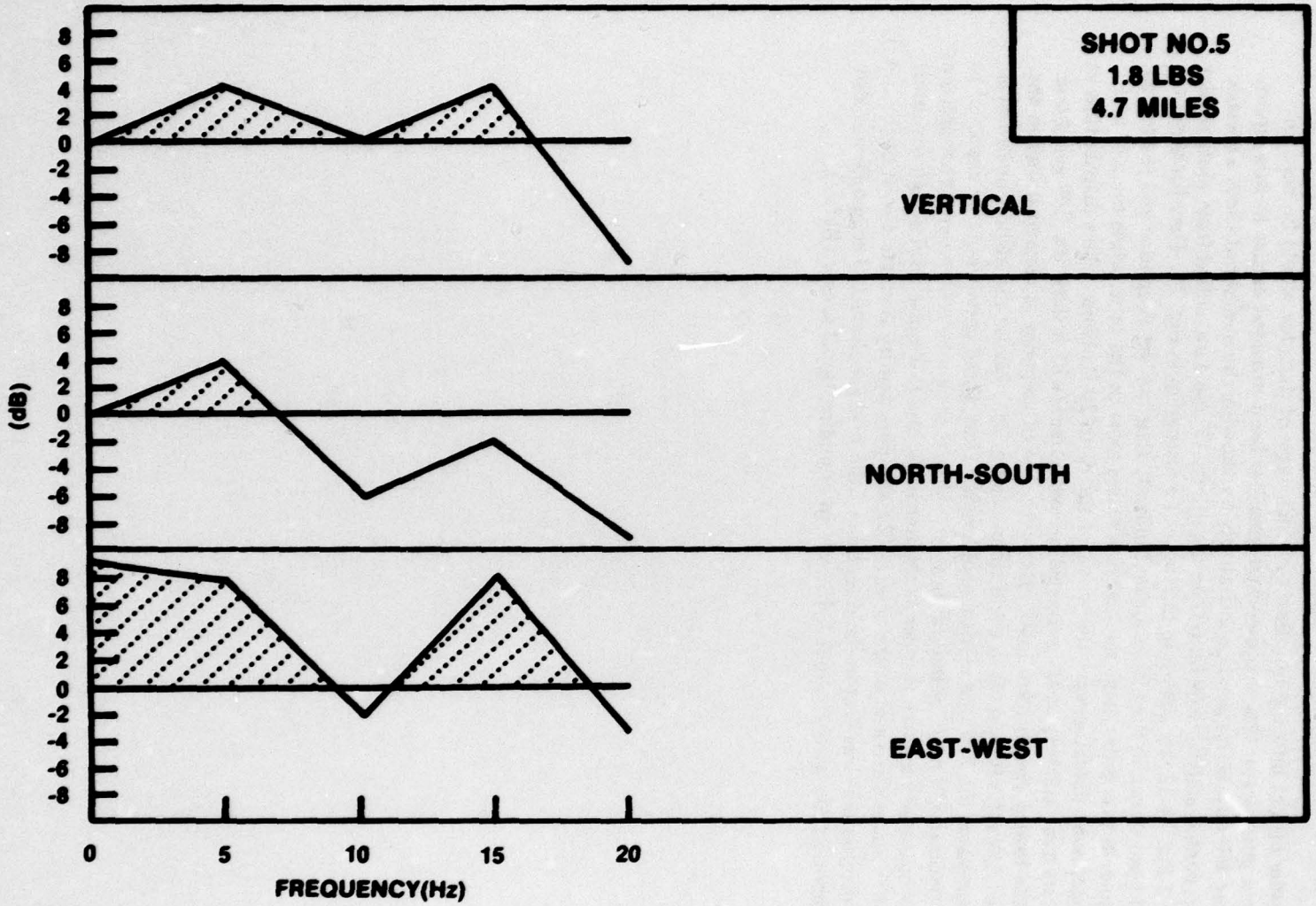

Figure 24. Seismic gain computed for 5 to 20 Hz. The null at 10 Hz may be due to poor coupling.

DISCUSSION AND INTERPRETATION

Some insight into the question of which type of detector would be best for surveillance purposes in this shallow-water area has been provided earlier in this report. The matter will now be resolved quantitatively by showing the number of times a specific detector recorded a higher S/N ratio than the others. These data, culled from plots similar to those of Fig. 18-22, are shown in the form of a histogram in Fig. 25. Data for shots 1 through 11 are shown in the histogram and indicate that the N-S geophone and the buried hydrophone, in that order, have the best S/N ratios most of the time, while the E-W and vertical geophone detector were the worst in the 5- to 20-Hz band. This distribution at first appears contradictory to the propagation loss curves (which show the E-W geophone to have the lowest propagation loss). However, the discrepancy is cleared up when the concept of S/N ratio is used (as in the histogram, Fig. 25) because the highest noise levels were observed on the E-W and vertical geophones. Thus, these units would be expected to have the poorest S/N ratio, as indeed they do. Also, it should be remembered that ambient noise propagates in the same manner as the signals, so the E-W noise level is high for three reasons: (1) surf noise is east of the tower; (2) shipping density is greatest west of the tower; and (3) propagation was best in the direction of the E-W geophones. The geophones also have a directionality gain of about 5 dB over an omnidirectional sensor (Ref. 2).

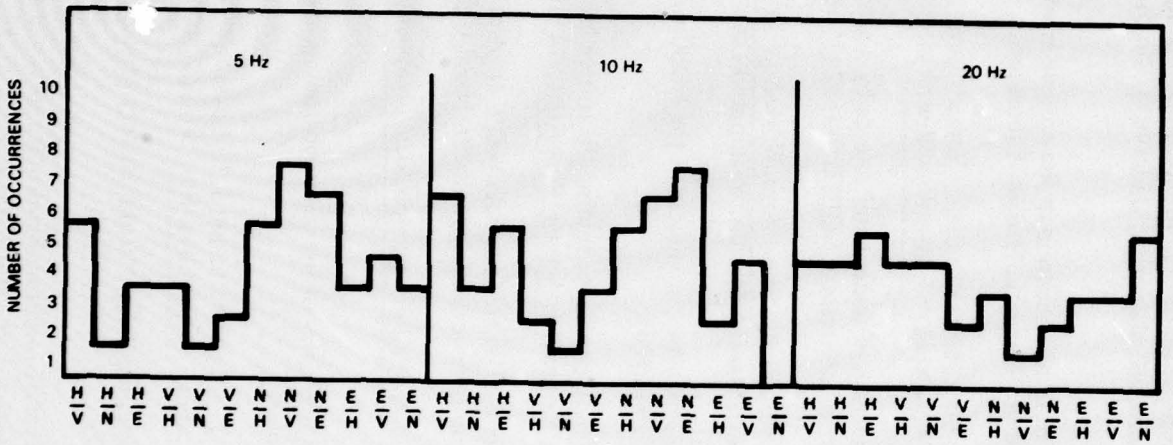

Figure 25. Histogram of the number of times the S/N ratio was greater on one detector than another. Data are for shots 3 through 11 and therefore include both the "ground" and "water" arrivals.

REFERENCES

1. R. J. Urick, Final Report: Seismic sensing of sounds in the sea, Tracor, Inc., 1601 Research Blvd., Rockville, MD 20850 (1971).

2. R. J. Hecht, Investigation of the potentialities of using seismic sensors for detection of ships and other naval platforms, Underwater Systems, Inc., Silver Spring, MD 20910 (1978).

3. M. Blaik and C. S. Clay, Detection in the ground of sound from a source in shallow water, Columbia University, Hudson Laboratories, Technical Report 76 (1959).

4. J. Northrop, M. Blaik, and C. S. Clay, "Some siesmic profiles onshore and offshore Long Island, New York," J. Geophys. Res., Vol. 64, 231 (1959).

5. R. J. Urick, Detection of underwater sounds by a geophone planted in the bottom, Naval Ordnance Laboratory, NOLTR 68-102 (1968).

6. Office of Naval Research, Proceedings, Workshop on Seismic Propagation in Shallow Water, Office of Naval Research, Washington D.C. (1978).

7. J. Northrop, Geoacoustic parameters of the NOSC tower site, Naval Ocean Systems Center, TN 529 (1978).

8. R. J. Urick, "Handy curves for finding the source level of an explosive charge fired at a depth in the sea," J. Acoust. Soc. Am., Vol. 49, 935 (1971).

9. W. H. Watson and R. W. McGirr, RAYWAVE II: A propagation loss model for the analysis of complex ocean environment, Naval Undersea Center, TN 1516 (1975).

10. M. B. Dobrin, Introduction to geophysical prospecting, McGraw-Hill, New York, N.Y. (1952).

11. G. J. Fryer, "Reflectivity of the ocean bottom at low frequency," J. Acoust. Soc. Am., Vol. 63, 35 (1978).

12. K. L. Cook, S. T. Algermissen, and J. K. Costain, "The status of PS converted waves in coastal studies," J. Geophys. Res., Vol. 67, 4769 (1962).

13. W. C. Cummings, San Diego Natural History Museum, personal communication, January 1979.

14. G. A. Clapp, Shallow water ambient noise survey at the NEL oceanographic tower, Naval Electronics Laboratory, TR 1115 (1962).

15. E. L. Hamilton, Shear wave velocity versus depth in marine sediments: a review, Geophysics, Vol. 41, 985 (1976).

16. H. W. Kutschale, Rapid computation by wave theory of propagation loss in the Arctic Ocean, Lamont-Doherty Geological Observatory, Columbia University, Technical Report 8, March, 1973.

INITIAL DISTRIBUTION

DEPARTMENT OF DEFENSE AGENCIES

DEFENSE ADVANCED RESEARCH
PROJECTS AGENCY
NMRO (DR RALPH ALEWINE)
NMRO (DR CARL ROMNEY)

DEPUTY UNDER SECRETARY OF DEFENSE R&E
(STRATEGIC & SPACE SYSTEMS)
CAPT HL BIXBY, USN

DEFENSE DOCUMENTATION CENTER (12)

DEPARTMENT OF THE NAVY

OFFICE OF NAVAL RESEARCH
ONR-463 (JG HEACOCK) (5)
ONR-463 (R ANDREWS)
ONR-222 (GL BOYER) (2)
ONR-461 (L JOHNSON)
ONR-465 (RG JOINER)
ONR-462 (DR JAMES BAILEY)
ONR-462M (J MINARD)
ONR-432 (DR SL BRODSKY)
ONR-1028 (F DIEMER)
ONR-222 (CDR E O'BRIEN)
ONR-483 (DR THOMAS PYLE)
ONR-22 (DR ALAN SYKES)

CHIEF OF NAVAL OPERATIONS
NOP-9520 (LCDR ERNEST YOUNG)
NOP-961C4 (LCDR WM COBB)
NOP-987P1 (DR JAAP BOOSMAN)
NOP-095E (ROBERT WINOKUR)

CHIEF OF NAVAL MATERIAL
NMAT-08T24 (GR SPALDING)

NAVAL SEA SEA SYSTEMS COMMAND
NSEA-034 (CAPT JW ORGAN)
NSEA-031 (HF MURPHY)

NAVAL ELECTRONIC SYSTEMS COMMAND
NELEX-320 (DR JOEL SINSKY)
NELEX-320 (JOHN CYBULSKI)
PME-124-60 (CAPT DB MURTON)

NAVAL UNDERWATER SYSTEMS CENTER
NEW LONDON LABORATORY
CODE 311 (JAMES GALLAGHER)

NAVAL OCEANOGRAPHIC OFFICE
CODE 3400 (WH GEDDES)
CODE 3441 (DR JOJI TOMEI)

NAVAL OCEAN RESEARCH AND
DEVELOPMENT ACTIVITY
CODE 200 (HE MORRIS)
CODE 320 (DR AUBREY ANDERSON)
CODE 320 (ROCKNE ANDERSON)
CODE 320 (MIKE STANLEY)
CODE 320 (STANLEY CHIN-BING)
CODE 320 (DR JAMES DAVIS)
CODE 340 (DR GERALD MORRIS)
CODE 360 (DR HERBERT EPPERT)
CODE 360 (JA BALLARD)
CODE 362 (JAMES MATTHEWS)

NAVAL POSTGRADUATE SCHOOL
CODE 61Sd (DR JV SANDERS)
CODE 61To (DR IVAN TOLSTOY)
CODE 61Me (DR PAUL MOOSE)
CODE 61Cz (DR AB COPPENS)

NAVAL COASTAL SYSTEMS CENTER
CODE 792 (DR E GLENN MC ELROY)
CODE 792 (R FIDLER)
CODE 792 (DR KEN ALLEN)

SACLANT ASW RESEARCH CENTER
DR DONALD ROSS, DEPUTY DIRECTOR

NAVAL RESEARCH LABORATORY
CODE 8130
CODE 8123 (CW VOTAW)
CODE 8160 (O DIACHOK)
CODE 8133 (DR JA BUCARO)
CODE 8133 (DR SAM HANISH)
CODE 8121 (DR A ELLER)
CODE 8109 (CARL R ROLLINS)
CODE 8120 (RAYMOND FERRIS)

NAVAL SURFACE WEAPONS CENTER
WHITE OAK LABORATORY
WR-41 (DR I BLATSTEIN)

DEPARTMENT OF THE AIR FORCE

AIR FORCE OFFICE OF SCIENTIFIC RESEARCH
WILLIAM BEST

VELA SEISMOLOGICAL CENTER
DR ROBERT ROTHMAN
CAPT MJ SHORE, USAF

OTHER GOVERNMENT (NON DOD)

GEOLOGICAL SURVEY, DEPT OF THE INTERIOR
DR RICHARD SILWESTER

NATIONAL SCIENCE FOUNDATION
DR ROY HANSON
DR DON HEINRICHS

UNIVERSITIES/INSTITUTIONS

APPLIED RESEARCH LABORATORY
PENNSYLVANIA STATE UNIVERSITY
NICK ABOUREZK

UNIVERSITY OF WAHSINGTON
ELECTRICAL ENGINEERING DEPT
DR RUBENS SIGELMANN
APPLIED PHYSICS LABORATORY
DR JA MERCER

UNIVERSITY OF TEXAS
APPLIED RESEARCH LABORATORY
DR LLOYD HAMPTON
DR KEN HAWKER

THE MARINE SCIENCE INSTITUTE OF THE
UNIVERSITY OF TEXAS
DR JOSEPH WORZEL
DR GARY LATHAM
DR H JAMES DORMAN
DR MARK HOUSTON

CORNELL UNIVERSITY
DEPT OF GEOLOGICAL SCIENCES
DR JACK OLIVER
DR BRYAN ISACKS

THE COURANT INSTITUTE OF
MATHEMATICAL SCIENCES
NEW YORK UNIVERSITY
DR DAVID STICKLER

THE LAMONT-DOHERTY GEOLOGICAL
OBSERVATORY OF COLUMBIA UNIVERSITY
ROBERT E HOUTZ
DR ROBERT STOLL
H KUTSCHALE

UNIVERSITY OF HAWAII
HAWAII INSTITUTE OF GEOPHYSICS
DR GEORGE SUTTON
DR DAN WALKER

SCRIPPS INSTITUTION OF OCEANOGRAPHY
MARINE PHYSICAL LABORATORY
DR GEORGE SHOR

WOODS HOLE OCEANOGRAPHIC INSTITUTION
DR JOHN EWING
DR EARL HAYES

UNIVERSITY OF CALIFORNIA' SAN DIEGO
IGPP (DR JM BRUNE)

SAN DIEGO STATE UNIVERSITY
GEOLOGY SCIENCE DEPT
RW BERRY

THE JOHNS HOPKINS UNIVERSITY
APPLIED PHYSICS LABORATORY
GENE BYRON

MASSACHUSETTS INSTITUTE OF TECHNOLOGY
LINCOLN LABORATORIES
DR THOMAS LANDERS
DR RICHARD LACOSS

COMPANIES (COMMERCIAL)

PLANNING SYSTEMS,
7900 WESTPARK DRIVE
MC LEAN, VA 22101
DR LOUIS P SOLOMON

POLAR RESEARCH LABORATORY
123 SANTA BARBARA STREET
SANTA BARBARA, CA 93101
B BUCK

TRACOR, INC.
1601 RESEARCH BLVD
ROCKVILLE, MD 20850
ROBERT URICK

UNDERWATER SYSTEMS, INC
8121 GEORGIA AVE
SILVER SPRING, MD 20910
DAN WOOLSTON
RICHARD HECHT

THE WESTON GEOPHYSICAL CORPORATION
P.O. BOX 550
WESTBOROUGH, MA 01581
ANDREW LECROIX

THE INSTITUTE OF ACOUSTIC RESEARCH
615 SW 2ND AVE
MIAMI, FL 33130
DR MORTON KRONENGOLD
DR DON FLETCHER

BOEING AEROSPACE COMPANY
TACTICAL SYSTEMS CONCEPTS
ADVANCED PROJECTS
P.O. BOX 3999, M.S. 84-63
SEATTLE, WA 98124
BOB ARNOLD
DWIGHT FUGIMOTO
RICHARD EDSINGER
DR KEITH NARSWORTHY
DR DONALD NELSON

ENSCO, INC.
5408A PORT ROYAL ROAD
P.O. BOX 1346
SPRINGFIELD, VA 22151
JAMES CALDWELL
LYNN ACKLER
JOHN GREEN